
[All ETDs from UAB](#)

[UAB Theses & Dissertations](#)

2002

Cardiac remodeling and systolic function in response to hypertension (HTN), diabetes (D), and hypertension-diabetes (H-D).

Juan Mario Bernal
University of Alabama at Birmingham

Follow this and additional works at: <https://digitalcommons.library.uab.edu/etd-collection>

Recommended Citation

Bernal, Juan Mario, "Cardiac remodeling and systolic function in response to hypertension (HTN), diabetes (D), and hypertension-diabetes (H-D)." (2002). *All ETDs from UAB*. 4818.
<https://digitalcommons.library.uab.edu/etd-collection/4818>

This content has been accepted for inclusion by an authorized administrator of the UAB Digital Commons, and is provided as a free open access item. All inquiries regarding this item or the UAB Digital Commons should be directed to the [UAB Libraries Office of Scholarly Communication](#).

INFORMATION TO USERS

This manuscript has been reproduced from the microfilm master. UMI films the text directly from the original or copy submitted. Thus, some thesis and dissertation copies are in typewriter face, while others may be from any type of computer printer.

The quality of this reproduction is dependent upon the quality of the copy submitted. Broken or indistinct print, colored or poor quality illustrations and photographs, print bleedthrough, substandard margins, and improper alignment can adversely affect reproduction.

In the unlikely event that the author did not send UMI a complete manuscript and there are missing pages, these will be noted. Also, if unauthorized copyright material had to be removed, a note will indicate the deletion.

Oversize materials (e.g., maps, drawings, charts) are reproduced by sectioning the original, beginning at the upper left-hand corner and continuing from left to right in equal sections with small overlaps.

ProQuest Information and Learning
300 North Zeeb Road, Ann Arbor, MI 48106-1346 USA
800-521-0600

UMI[®]

CARDIAC REMODELING AND SYTOLIC FUNCTION IN RESPONSE TO
HYPERTENSION (HTN), DIABETES (D), AND HYPERTENSION-DIABETES
(H-D)

by

JUAN MARIO BERNAL

A THESIS

Submitted to the graduate faculty of The University of Alabama at Birmingham,
in partial fulfillment of the requirements for the degree of
Master of Science

BIRMINGHAM, ALABAMA

2002

UMI Number: 1411126

Copyright 2002 by
Bernal, Juan Mario

All rights reserved.

UMI[®]

UMI Microform 1411126

Copyright 2002 by ProQuest Information and Learning Company.
All rights reserved. This microform edition is protected against
unauthorized copying under Title 17, United States Code.

ProQuest Information and Learning Company
300 North Zeeb Road
P.O. Box 1346
Ann Arbor, MI 48106-1346

Copyright by
Juan Mario Bernal
2002

ABSTRACT OF THESIS
GRADUATE SCHOOL, UNIVERSITY OF ALABAMA AT BIRMINGHAM

Degree M.S.BMS. Program Basic Biomedical Sciences

Name of Candidate Juan Mario Bernal

Committee Chair Kathleen H. Berecek

Title Cardiac Remodeling and Systolic Function in Response to Hypertension (HTN),
Diabetes (D), and Hypertension-Diabetes (H-D)

In the United States, heart failure (HF) affects more than 4.7 million people with over half a million new cases each year. Hypertension (HTN) and Diabetes Mellitus (DM) are both independent risk factors for the development HF. Both DM and HTN have a deleterious effect on the heart muscle resulting in a steady decrease in the ability of the heart to pump efficiently. The Extracellular Matrix (ECM) provides structural integrity and defines the architecture of the myocardium regulating mechanical properties and cardiac function. Changes in ECM homeostasis are affected by both DM and HTN through alterations in its constituents such as collagen, fibronectin, and proteoglycans. This study was designed to determine the differential temporal progression of LV remodeling and cardiac function in response to DM, HTP and HTN-DM, evaluating systolic function, LV geometry and cardiac ultrastructure. Our results showed that hyperglycemia caused a significant impairment in systolic function and adverse LV remodeling at 4 and 12. In addition, there was an increase in interstitial collagen deposition. HTN resulted in no significant changes in systolic function. However, LVH was evident at 6 and 12 weeks in addition to a significant increase in interstitial collagen deposition. Our results suggest that when HTH and DM were combined adverse

ventricular remodeling seemed to occur at a slower rate than that seen in the diabetic hearts alone. However, systolic function remained impaired at 6 and 12 weeks. Also H-D animals presented areas of replacement fibrosis in the endocardium.

We conclude that hyperglycemia caused a significant impairment in systolic function with adverse LV remodeling. It also produced an increase in interstitial collagen deposition at 4 and 12 weeks. HTN resulted in LVH and increase collagen deposition. Additionally, the combination of DM and HTN produced the most severe degree of interstitial fibrosis and replacement fibrosis. These results have led us to hypothesize that the compensatory response trigger by high blood pressure and the activation of RAS may play a role in preserving LV geometry in the diabetic heart, protecting against the adverse LV dilatation seen during diabetic cardiomyopathy. These mechanisms appear to be early and transitory phenomenon.

DEDICATION

This thesis is dedicated to my family and Ann Marie. To my family, thank you for giving me access to exceptional role models and teaching me the value of education, hard work and responsibility. To Ann Marie, thank you for your patience and for giving me love and support throughout these two years.

ACKNOWLEDGMENTS

I thank the members of my graduate committee, Drs. Kathleen H. Berecek, Pamela A. Lucchesi, Louis J. Dell'Italia, Gilbert J. Perry, and C. Roger White for their time, helpful suggestions and guidance during the course of this work. I would also like to thank all of those who taught me the different techniques necessary to complete this project.

TABLE OF CONTENTS

	<i>Page</i>
ABSTRACT.....	iii
DEDICATION.....	v
ACKNOWLEDGMENTS	vi
LIST OF TABLES.....	ix
LIST OF FIGURES	x
LIST OF ABBREVIATIONS.....	xi
INTRODUCTION	1
BACKGROUND	6
Diabetes.....	6
Alterations in systolic function	7
Structural changes	8
Alterations in cardiac metabolism	9
Hypertension.....	10
Alterations in systolic function.....	12
Left ventricular hypertrophy	12
Combined effects of diabetes and hypertension	13
Alterations in cardiac function.....	14
Alterations in cardiac structure	15
Anatomical and functional effects on the vascular bed	16
MATERIALS AND METHODS.....	18
Animals.....	18
Abdominal Aortic Coarctation.....	18
Diabetes induction	19
Hemodynamic measurements	20
Echocardiographic-Doppler studies.....	20
Determination of volume percent collagen.....	22
Immunohistochemistry	23
Statistical analysis.....	23

TABLE OF CONTENTS (Continued)

	<i>Page</i>
RESULTS.....	24
General characteristics of the animal groups	24
Hemodynamic measurements	24
Left ventricular remodeling.....	26
Systolic function.....	31
Interstitial collagen deposition	32
Immunohistochemistry.....	32
DISCUSSION	44
LIST OF REFERENCES	50
APPENDIX: INSTITUTIONAL ANIMAL CARE AND USE COMMITTEE APPROVAL FORM.....	59

LIST OF TABLES

<i>Table</i>	<i>Page</i>
1 Echocardiographic measurements of S, D, H, and H-D animals at 4 and 6 weeks	25
2 Echocardiographic measurements of S, D, H, and H-D animals at 12 weeks	25
3 Body and Heart weight obtained from S, D, H, and H-D animals at 4 and 6 weeks. HW and LV were normalized to BW for all groups	26
4 Body and Heart weight obtained from S, D, H, and H-D animals at 12 weeks. HW and LV were normalized to BW for all groups	27
5 Interstitial collagen deposition in the endocardium and epicardium of S, D, H, and H-D animals at 4 and 6 weeks	27
6 Interstitial collagen deposition in the endocardium and epicardium of S, D, H, and H-D animals at 12 weeks	27

LIST OF FIGURES

<i>Figure</i>	<i>Page</i>
1 Schematic representation of the gross morphological changes to the Heart wall during the progression to heart failure.....	1
2 Diagram representing the study design	5
3 Temporal progression of relative wall thickness (RWT).....	28
4 Relation of the velocity of circumferential shortening corrected for rate (VCFr) and circumferential stress	29
5 Calculated vertical distance (VD) from the regression line	30
6 Changes in interstitial collagen deposition found in the diabetic hearts	34
7 Focal fibrotic areas in the endocardium of H and H-D animals.....	36
8 Total interstitial collagen deposition in the myocardium.....	38
9 Temporal progression on interstitial collagen deposition in the myocardium.....	39
10 Immunohistochemical staining of rat myocardium for collagen type I.....	40
11 Immunohistochemical staining of rat myocardium for collagen type III	42

LIST OF ABBREVIATIONS

ACC	Abdominal aortic coarctation
AGE	Advanced glycosylation end product
ATPase	Adenosine triphosphatase
BW	Body weight
CMAP	Carotid mean arterial pressure
CO	Cardiac output
CVD	Cardiovascular disease
D	Diabetic animal
DM	Diabetes mellitus
ECM	Extracellular matrix
EjT	Ejection time
GRA	Glucocorticoid-remediable aldosteronism
H	Hypertensive animal
H-D	Hypertensive-diabetic animal
HF	Heart failure
HTN	Hypertension
HW	Heart Weight
IFG-1	Insulin growth factor - 1
ip	Intraperitoneal
IVS	Intraventricular septum

LIST OF ABBREVIATIONS (Continued)

LV	Left ventricle
LV/BW	Left ventricular weight / body weight
LVEDD	Left ventricular end-diastolic dimension
LVEDP	Left ventricular end-diastolic pressure
LVESD	Left ventricular end-systolic dimension
LVH	Left ventricular hypertrophy
LVM	Left ventricular mass
MMPs	Matrix metalloproteinases
MAP	Mean arterial pressure
mRNA	messenger ribonucleic acid
NE	Norepinephrine
PKC	Protein Kinase C
PWT	Posterior wall thickness
RAS	Renin angiotensin system
RWT	Relative wall thickness
S	Sham animal
STZ	Streptozocitin
TGF - β	Transforming growth factor - β
TIMPs	Tissue metalloproteinases inhibitors
VCFr	Rate-corrected velocity of circumferential shortening
VD	Vertical Distance
VLDL	Very low density lipoprotein

LIST OF ABBREVIATIONS (Continued)

WKY

Wistar-Kyoto

INTRODUCTION

In the United States, heart failure (HF) affects more than 4.7 million people with over half a million new cases each year¹. Hypertension (HTN) and Diabetes Mellitus (DM) are both independent risk factors for the development of HF. It is estimated that 50 million people over the age of 60 have HTN or are taking antihypertensive medication². In addition, DM alone is the fifth cause of death in the United States. Both DM and HTN have a deleterious effect on the heart muscle, resulting in a steady decrease in the ability of the heart to pump efficiently. This results in a wide spectrum of symptoms and clinical signs that lead to poor quality of life and increased health care costs.

Whether heart muscle damage is secondary to myocardial infarction, chronic ischemia, inflammation, pressure overload, or diabetes, there is a complex sequence of compensatory events that ultimately result in an adversely remodeled myocardium and a dilated, thin-walled, spherical ventricle, categorized into three stages as shown in Fig 1.

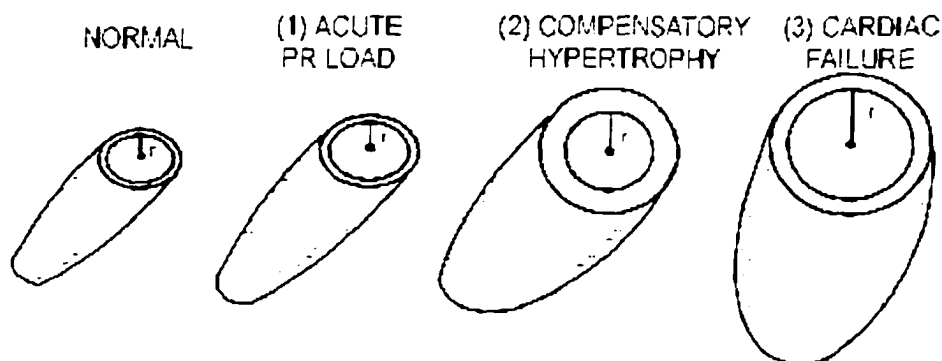


Figure 1. Schematic representation of the gross morphological changes to the heart wall during the progression to heart failure.

First, during acute preload, there is an increase in diastolic pressure with some compensatory myocyte hypertrophy and dramatic changes in extracellular matrix (ECM). Second, during compensatory hypertrophy, myocyte growth and ECM accumulation lead to an increase in ventricular wall thickness and chamber diameter. Nevertheless, there is a complex sequence of compensatory events resulting in a continual state of remodeling mediated by changes in myocyte morphology and in the ECM.

The ECM is in a dynamic state determined by matrix metalloproteinases (MMP) and their tissue inhibitors of metalloproteinases (TIMPs). MMPs are proteolytic enzymes that have been implicated in left ventricular (LV) dilatation in the progression to end-stage HF, presumably by excessive degradation of ECM. Changes in ECM homeostasis are affected by both DM³ and HTN⁴ through alterations in its constituents, such as collagen, fibronectin, and proteoglycans. This alters the interstitial network that provides the scaffolding of the cardiac myocytes that serves to direct, propagate, and distribute the contractile force of the whole heart. Numerous studies have documented that uncontrolled activity of MMPs is a key element in the abnormal ECM degradation leading to the development of severe HF, suggesting that heightened ECM degradation may contribute to the LV remodeling that occurs during the evolution of LV dilatation and HF.

Collagens constitute 3% to 6% of the myocardial weight and are produced predominately by fibroblasts. The 2 major collagen subtypes found in the heart are: type I and type III⁵. Type I collagen is arranged in thick parallel rod-like fibers and is found in large amount in tissues that require great tensile strength, such as bone and tendon. On the other hand, type III collagen forms a network of fibrils and is found in tissues where

highly elastic properties are needed, such as skin, blood vessels, and lungs. The proportion between these 2 components in the myocardium varies throughout the course of any hemodynamic stress and is considered to play a role in various pathological conditions, such as dilated cardiomyopathy, with cardiac fibrosis being an end-stage manifestation of HF in both HTN and DM.

Untreated, LV remodeling results in a progressive dilatation characterized by a disproportionate decrease in the ratio of LV wall thickness to diameter ratio, increase in myocardial wall stress, and development of HF. Therefore, it is of clinical importance to diagnose individuals with HTP and DM as early as possible in order to establish an adequate therapy targeted to reduce the risk of developing HF, its symptomatology, complications, and the number of cardiovascular events.

Consequently, an *in vivo* study of the temporal progression of cardiac remodeling and performance in response to HTN and DM, and the role of collagen changes on this adaptation, might reveal early alterations that modulate cardiac remodeling and might affect the initial adaptive response, that preserves a normal systolic function (Figure 2).

To investigate this response the current study was based upon the following hypothesis:

1. There is a differential temporal progression of LV remodeling in response to DM and HTP.
2. The combination of DM and HTN result in augmentation of adverse LV remodeling and systolic dysfunction.
3. In spite of the early differences in remodeling, both HTN and DM result in a progressive interstitial fibrosis.

4. The combination of DM and HTN result in an earlier and greater degree of interstitial fibrosis and modulation of LV remodeling compared to these stresses alone.

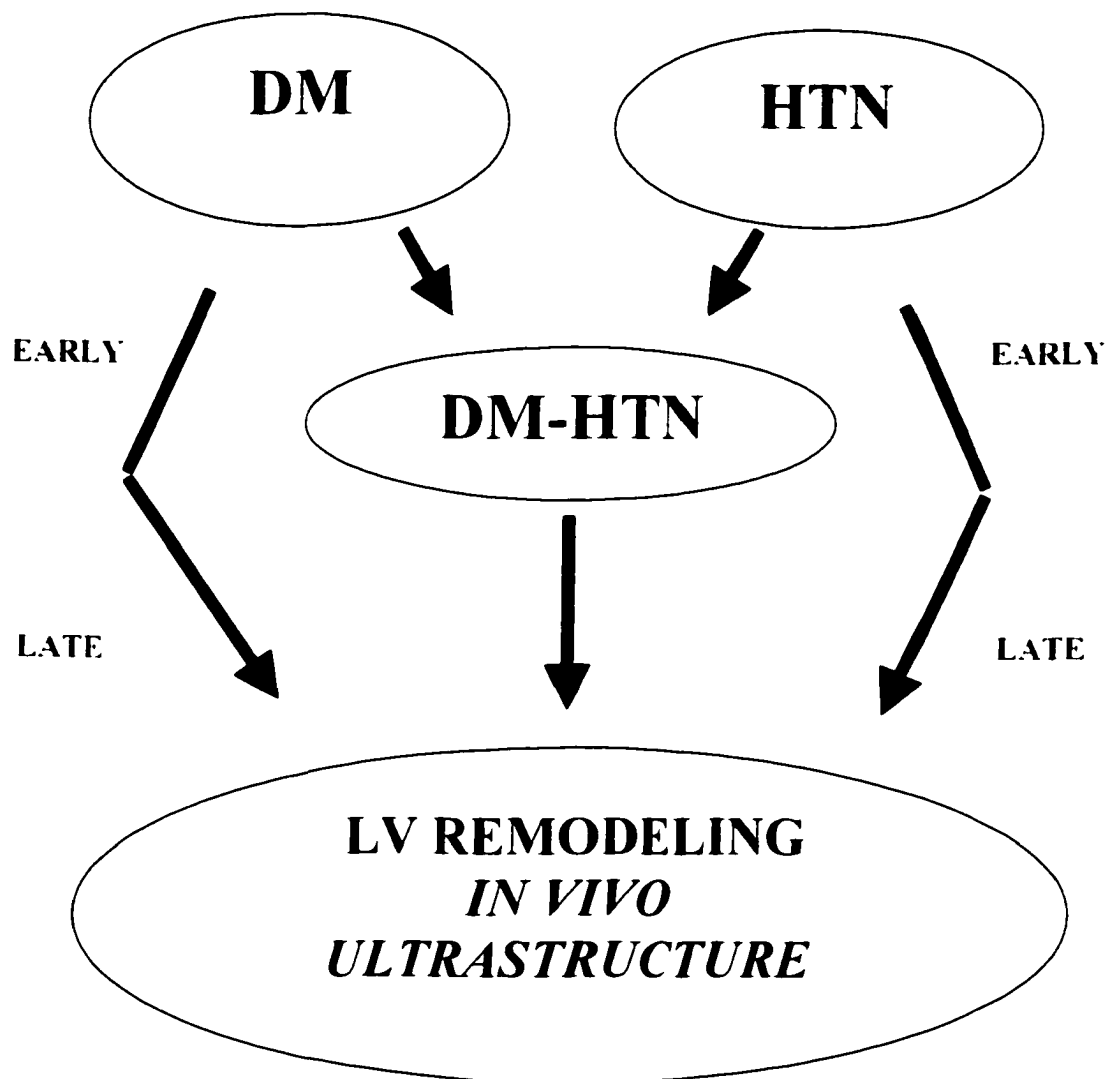


Figure 2. Diagram representing the study design.

BACKGROUND

Diabetes. DM is the most common chronic endocrine disease. It is a chronic disease characterized by metabolic derangements consisting of hyperglycemia, hypoinsulinemia, and electrolyte imbalances. These metabolic derangements are accompanied by such characteristic, long-term complications as neuropathy, nephropathy, and vasculopathy.

Clinically, the disease is classified into the following four major groups. Type I Diabetes accounts for 5% to 10% of cases in the United States. It is characterized by the destruction of the pancreatic β cell islets, which produces insulin deficiency. The destruction of these cells is either immune-mediated or idiopathic. Type 2 Diabetes accounts for 90% to 95% of cases in the United States. During its development, insulin sensitivity ranges from insulin resistance to insulin deficiency. The third major group is gestational diabetes mellitus. Fourth, there are other specific types, some of which are drug- or infection-induced. Among the most significant long-term complications of DM are retinopathy, nephropathy, neuropathy, and cardiomyopathy⁶. It is estimated that 10.4 million Americans have DM. From those, 4.8 million are males and 5.7 million are females⁷. The association of diabetes with other cardiovascular risk factors leads to increased morbidity, mortality, and costly consequences to the health system.

The Framingham study showed that the incidence of cardiovascular disease, as well as the levels of cardiovascular risk factors, were higher in diabetic than in non-diabetic individuals. Furthermore, the increase in mortality and incidence of HF seen in

diabetic patients was higher in women than in men⁸. Indeed, cardiovascular mortality is two or three times higher in men with DM and three to five times higher in women with DM than in counterparts without it⁸⁻¹⁰.

Alterations in systolic function. Systolic function in diabetic animals has been evaluated in different *in vivo* and *in vitro* studies. In addition, population-based studies, have shown that DM alone is associated with an impaired systolic chamber function and is independent of age, gender, body mass index, and heart rate¹¹.

Studies in isolated myocytes have shown intrinsic contractile dysfunction in response to hyperglycemia¹². Myocytes from diabetic rats exhibited decreased shortening, reduced maximum rates of shortening and relengthening, and prolonged time to peak shortening¹³. Likewise, Ca²⁺ handling by the sarcoplasmic reticulum was impaired, with a delay in cardiac uptake and decreased ATPase activity¹⁴. These alterations modify Ca²⁺ stores and produce an overall alteration in chamber performance. Furthermore, alterations in K⁺ channel¹⁵⁻¹⁷, Na⁺-Ca²⁺ exchanger activities¹⁸ and abnormalities in protein kinase C (PKC) metabolism¹⁹ have also been proposed as underlying mechanisms for these alterations.

Studies of the effects of the diabetic state on cardiac function *in vivo*¹² or in isolated perfused heart preparations²⁰ have been contradictory. Using Streptozocitin (STZ) to induce pancreatic β cell destruction and hyperglycemia, several studies have shown that systolic function determined by maximal dp/dt and LV peak systolic pressure remained within normal limits at 8 weeks after STZ administration²¹. Another study showed that after 5 weeks of STZ injection these indexes were decreased when compared

to control¹². In addition, others have shown that the cardiac response to sympathetic stimulation by norepinephrine (NE) administration was significantly diminished²¹. Moreover, it has been proposed that the reduction in the number of β_1 receptors on cardiac tissue²², as well as the impairment in the coupling of the receptor to the second messenger^{22,23} may underline the attenuation in the cardiac response to inotropic and chronotropic agents like dobutamine^{24,25}.

Structural changes. Structural changes in the heart have been postulated as the main determinants in the mechanisms underlying cardiac dysfunction in experimental diabetes as well as in diabetic individuals. Changes in collagen contribute in part to the deleterious effects of this disease. Collagen is a major component of the ECM that provides structural integrity and defines the architecture of the myocardium, and regulates both mechanical properties and cardiac function. Increases in total collagen deposition have been described in the hearts of diabetic humans³ and mice²⁶. However, studies in STZ treated rats have shown no increase in total collagen deposition when compared to controls^{29,27,28}. These results clearly suggest a species variant response to multiple stimuli-inducing collagen synthesis. Insulin, insulin growth factor 1 (IGF-1), and the renin angiotensin system (RAS) have been proposed to regulate in some extent these collagen changes.

In addition to interstitial fibrosis, the accumulation of advanced glycosylation end products (AGEs) cause an increase in collagen cross-linking and a reduction in solubility that may also influence the passive-elastic properties of the heart, leading to a stiffer myocardium²⁸. Accumulation of AGEs in the vascular tissue has been proved to be

related to the degree of vascular disease seen in diabetic patients²⁹. These products induce vascular proliferation and protein synthesis by acting through a membrane-associated macrophage receptor that consequently releases tumor necrosis factor and interleukin-1²⁹.

Another important structural change occurring in the diabetic myocardium results from a shift in myosin isoenzyme from V1 to V3, which leads to a decrease in cardiac myosin-ATPase activity. These alterations in structural and functional proteins play an important role in the functional impairment seen in the development and complications of diabetic cardiomyopathy

Alterations in cardiac metabolism. The myocardium is highly dependent on ATP production by the mitochondria. The substrates for this production include glucose, lactate, free fatty acids, and ketone bodies. Glycolysis provides a high percentage of substrates for the production of ATP. In addition, fatty acids also provide an important percentage of substrates, especially in the rat. During diabetes, the alterations in lipid and glucose metabolism compromise the quality and quantity of energy supplies to the heart. First, there is a decrease in carbohydrate utilization via the glycolytic pathway, as well as an increased glycogen utilization³⁰. Second, there is a reduction in glucose transport, which is due to a reduction in the insulin-sensitive transporter (GLUT 4) in the myocytes^{31,32}.

Finally, intracellular utilization of glucose is reduced due to impaired phosphorylation mechanisms and the depression of the pyruvate dehydrogenase pathway³³ with an overall decrease in glucose oxidation.

Lipid metabolism is also compromised in diabetic patients and, most importantly, is a strong predictor for cardiovascular disease³⁴. Lipolysis is a metabolic pathway that provides fatty acids and glycerol. During diabetes the activity of the rate-limiting enzyme is no longer under inhibition, leading to excessive lipolysis³⁵. Additionally, in DM the activity of the endothelial enzyme lipoprotein lipase is reduced due to the insulin deficiency in both rats and humans^{36,37}. Thus, very low-density lipoproteins (VLDL) levels increase with subsequent alteration in the free fatty acid metabolism.

Intracellularly, the depletion of carnitine seen in the diabetic hearts³⁸ compromises not only β oxidation of long chain fatty acids but also cellular integrity, due to the accumulation of free fatty acids and their intermediates, leading to myocardial cell dysfunction^{39,40}.

Hypertension. HTN is a well-known risk factor in the development of cardiovascular disease (CVD)⁴¹. Amongst the most severe manifestations of CVD, HF is the major contributor to cardiovascular morbidity and mortality in the United States⁴². It is also a predisposing factor for the development of peripheral vascular disease, stroke, and renal disease. Currently in the US, it is estimated that 50 million people over the age of 60 have HTN or are taking antihypertensive medication². However, the distribution varies with multiple factors, such as race, age, geographic patterns, gender, and socioeconomic status. HTN has classically been categorized into essential and secondary HTN. Secondary forms of HTN are correctable forms of high blood pressure, whereas in essential HTN the causes are often unknown. In addition, essential HTN is a polygenic disease in which overexpression and underexpression of different genes have been

identified over the last several decades⁴³. Mutations in at least 10 genes have been shown to affect blood pressure through a common pathway by affecting salt homeostasis and water balance^{44,45}. Among those, glucocorticoid-remediable aldosteronism (GRA), Liddle's Syndrome, and apparent mineralocorticoid excess are the most studied.

Another important mechanism that contributes to the pathogenesis of HTN involves alterations in RAS. Numerous experimental models of pressure overload have been used to study the effect of high blood pressure in the heart. As early as 1938, authors reported the use of abdominal aortic constriction for the induction of HTN. The major pathophysiologic mechanism underlying this model is the activation of the RAS⁴⁶. This model is characterized by a sustained elevation of systolic blood pressure that appears approximately after 2 weeks and remains elevated for periods as long as 20 weeks⁴⁷. In addition to producing a sustained elevation in blood pressure, this model increases left ventricle /body weight ratio (LV/BW) ratio, and wall thickness in systole and diastole. One of the most important applications of this model has been its use in the study of cardiovascular effects of HTN and DM.

Alterations in systolic function. Early clinical studies showed that systolic dysfunction occurred very late in the course of hypertensive heart disease^{48,49}. However, recent studies using more sophisticated methods have demonstrated that at least 15% of hypertensive individuals showed an impaired LV systolic function⁵⁰. One of the distinctions of the hypertrophied heart is its inability to increase end-diastolic volume during exercise. Hence, an increase in load, such as that seen during exercise, may reveal systolic abnormalities in hypertensive patients whose systolic performance at rest was

normal^{51,52}. In addition, when decreased ejection fraction and fractional shortening were present, a positive correlation between abnormal diastolic filling patterns and these parameters was found⁵³.

Experimental models of renal HTN in rats have shown that hemodynamic determinations of maximal rate of pressure generation (positive dp/dt) did not differ from the control groups during a 30-week observation period⁵³. On the other hand, other authors have reported that LV peak pressure as well as dp/dt was increased after 4 and 8 weeks during the development of left ventricular hypertrophy (LVH)⁵⁴. Investigators using the ascending aorta model have shown a hyperdynamic left ventricle when endocardial shortening was evaluated. However, when midwall shortening was assessed, LV systolic function was decreased after 6 weeks⁵⁵.

Left ventricular hypertrophy. LVH develops in response to high blood pressure. It involves an increase in the extracellular matrix components (myocardial fibrosis) as well as an increase in myocyte size (hypertrophy)^{4,56}. During the development of LVH, the collagen ratio undergoes constant changes. Procollagen type III messenger ribonucleic acid (mRNA) can be detected early (4 weeks) after abdominal aortic coarctation and persists for a long period of time (16 weeks), whereas the levels of procollagen type I mRNA increased after 16 weeks of chronic overload¹².

LVH plays a major role in the heterogeneous environment of regulatory and compensatory mechanisms in which HF develops. Therefore, when compensatory mechanisms saturate, manifestations of HF occur. The development of LVH involves a complex interaction among multiple factors, including hemodynamic constituents,

regulatory systems such as RAS^{57,58}, catecholamines, and genetic determinants. As previously described, the development of LVH has been classically characterized in 3 stages. Clinical studies have shown that the prevalence of LVH in populations with moderate essential HTN was 12-30%, as determined by echocardiography⁵⁹⁻⁶¹. In individuals with severe or malignant HTN the prevalence of LVH may exceed 90%^{62,63}. LVH has been clearly established to be a strong independent risk factor for cardiovascular morbidity and mortality⁶²⁻⁶⁴. Several mechanisms have been described for this predisposition. These include a reduction of coronary flow reserve, secondary to increased demand and/or altered microvascular function⁶⁵ and the induction of arrhythmias^{66,67}.

Combined effects of diabetes and hypertension. DM and HTN are both major causes of morbidity and mortality with costly implications to the health system. It is estimated that more than 3 million Americans have this ominous combination⁶⁸. There is strong evidence that this combination has an additive detrimental effect on the cardiovascular system as well as other systems⁶⁹⁻⁷¹. It has been demonstrated that HTN occurs twice as frequently in individuals with DM as in individuals without it⁷². Experimental studies examining the combined effect of renovascular HTN and diabetes have shown significant changes in myocardial function and structure⁷³, among alterations in other systems. Characteristics of this experimental animal model include the increase in mortality associated with circulatory congestion, evidenced by an increase in relative lung weight as well as liver weight⁷⁴. In addition, the distinctive effect of DM on body weight is even more pronounced in animals with a combined pathology^{73,74}.

Alterations in cardiac function. The deleterious effects of this combination have been positively identified in the myocardium, whether manifested as systolic or diastolic dysfunction^{70,75}. Previous studies⁷¹ have found that LV diastolic abnormalities are more frequent and greater in diabetic patients with HTN than in those without it. Early studies⁷⁶, focusing on the clinical features of hypertensive-diabetic individuals showed that these patients had long history of peripheral vascular disease and heart failure. Moreover, recent population-based studies¹¹ have shown that LV systolic function was decreased by 18% in hypertensive-diabetic individuals when compared to non-affected counterparts. However, cardiac output and cardiac index remained unchanged.

The prevalence of diastolic dysfunction has been documented to be as high as 44% when these two risk factors are present⁷⁷. Most importantly, these abnormalities have been positively correlated to the degree of fibrosis seen in hypertensive-diabetic individuals²⁷. Experimental⁷⁸ as well as clinical studies in hypertensive individuals have demonstrated that the regression of cardiac fibrosis improves diastolic performance⁷⁹.

Experimental models using isolated heart preparations have found that hypertensive-diabetic hearts had decreased contractility, with lower aortic output, coronary flow, and cardiac output (CO)⁶⁹. Additionally, functional studies using isolated papillary muscle showed that the contraction and relaxation times were increased in hypertensive diabetic hearts⁷⁴.

Electrophysiological abnormalities are also potential mechanisms affecting cardiac function and stability when these two diseases are combined. Studies have shown that the resting membrane potential and amplitude were decreased. Furthermore, action

potential duration was increased significantly in hypertensive-diabetic (H-D) animals⁷⁴. In addition to presented during diabetes alone, in the hypertensive-diabetic hearts, Ca^{2+} myosin ATPase activity decreases. In addition, the V1 myosin isoenzyme was also decreased. These changes in functional proteins have been found to have a good correlation with the degree of dysfunction seen in an isolated papillary muscle study⁷⁴.

Alterations in cardiac structure. Changes in LV geometry produce devastating deleterious effects on normal cardiac physiology and function. In humans, both HTN and diabetes have effects on LV geometry, with diabetes producing a significant increase in left ventricle relative wall thickness (RWT), and with HTN inducing a significant increase in LV mass¹¹. These modifications translate into the presence of LVH, with a consequent increase in the number of cardiovascular events. In addition to severe geometry changes, the presence of fibrosis is also evident. Myocardial fibrosis and scarring in H-D individuals were significantly increased when compared to patients with diabetes or HTN alone. In addition, there was the presence of frequent myocytolytic areas⁷⁶. Likewise, DM has summative effects by not only augmenting cardiac fibrosis and cardiac hypertrophy⁸⁰, but also by accelerating the development of LVH in patients with HTN⁸¹. Post-mortem studies examined the hearts of diabetic, hypertensive, and H-D patients⁸² have demonstrated that the greatest increase in mean HW and interstitial fibrosis was in the H-D patients. More recent studies have shown that HTN and diabetes act additively on LV wall thickness and total mass¹¹.

Anatomical and functional effects on the vascular bed. Even though diabetic cardiomyopathy has been identified in the absence of coronary artery disease, alterations in the microvasculature have been demonstrated to play a role in the pathophysiology of this combination.

First, animal studies have shown that H-D rats presented pronounced areas of microvascular tortuosity, arteriolar constriction, and microaneurysm formation⁸³. Second, impaired vascular relaxation and increased vasoconstriction are major functional abnormalities observed in microvasculature of hypertensive diabetic patients. Normal endothelium function is impaired during HTN as a response to the increasing shear forces and dysregulation of homeostatic mechanisms that control relaxation, platelet aggregation, and cell growth. Additionally, high glucose concentrations decrease endothelium-derived factor relaxation and increase vasoconstriction and vascular smooth muscle cell proliferation^{84,85}. Furthermore, the increased vascular leakiness seen in the diabetic microcirculation might be enhanced by the increased permeability seen in the dilated microcirculatory segments of hypertensive animals⁸³. These alterations in permeability result in leakage of cells and plasma components into the extravascular compartment, which results in the release of various cytokines and growth factor leading to abnormal accumulation of ECM components^{83,86,87}.

Abnormalities seen in platelet aggregation have striking effects on the morbidity and mortality of patients with DM and HTN. During normal platelet function, the homeostasis between Ca^{2+} and Mg^{2+} is critical for adequate platelet aggregation. Both DM and HTN elevate Ca^{2+} and decrease Mg^{2+} , producing an ionic imbalance that might contribute to enhanced platelet aggregation^{88,89}. In addition, when diabetes and HTN are

associated with high levels of factor VIII and PAI-1. the coagulation cascade diverts towards the procoagulant state.

MATERIALS AND METHODS

Animals. Male, Wistar Kyoto rats (WKY), 250-300 gm, were used for all studies. Animals were purchased from Harlan breeding laboratories and bred at the University of Alabama at Birmingham Animal Research Center. Twenty-seven female and nine male WKY were bred per year. Breeders were replaced at 4-6 month intervals. Animals were maintained and handled in accordance with the National Research Council Guide for the Care and Use of Laboratory Animals, and experiments were approved by the University of Alabama at Birmingham Institutional Animal Care and Use Committee. Animals were housed 4 per cage in temperature-controlled rooms on a 12-hour light-dark cycle and were given food and water ad libitum. When animals reached 250-300 gm, they were randomly selected into four different groups: Sham (S), Hypertensive (H), Diabetic (D) and Hypertensive Diabetic (H-D).

HTN was induced by abdominal aortic coarctation (AAC), and DM was induced by STZ injection. Animals were studied at 4, 6, and 12 weeks after AAC and/or STZ injection and S intervention. Hemodynamic measurements, cardiac function, and cardiac collagen analysis were evaluated at 6 weeks after AAC and AAC + STZ injection, after 4 weeks for STZ injection alone, and after 12 weeks for AAC, STZ injection alone, and AAC + STZ.

Abdominal Aortic Coarctation. AAC was performed using a modified method from that previously described⁹⁰. This model is characterized by an early and sustained

elevation in mean arterial pressure (MAP) in which the RAS plays an important role in triggering the development of LVH⁴⁷.

WKY rats between 250-275 g were anesthetized with ketamine (80-100 mg/kg) plus xylazine (5 mg/kg) ip. Under sterile conditions, the abdominal cavity was opened via a midline incision. The abdominal aorta and both renal arteries were exposed. Partial constriction of the abdominal aorta between the renal arteries was made using a Small Hemoclip (Weck, Inc.) set to an internal diameter of 0.45 mm. The peritoneal cavity was closed with coated VICRYL (Ethicon, Inc.), and the skin was closed with metallic clips. Sham-animals experienced the same surgical procedure without the clip placement. Animals were placed on a 37°C heating pad for the duration of the surgery and were allowed to recover, while the researcher monitored movement, water, and food intake.

Diabetes induction. Animals were given a single ip injection of STZ 60 mg/kg (Sigma, St Louis) dissolved in citric buffer pH 4.6. STZ is an antibiotic extracted from *Streptomyces achromogenes*, which causes β -cell degranulation and necrosis-producing chronic hyperglycemia and hypoinsulinemia. When intermediate doses (55–65 mg/kg) are used, no insulin is required for survival. Injected animals were fasted for 12 hours, and blood glucose was determined 1 week after STZ injection. Sham-animals were injected citric acid buffer pH 4.6 alone. Only animals that had glucose levels above 250 mg/dl were included in the D group. Initial blood glucose determination was done after 7 days and obtained from tail vein samples using a blood glucose meter, equipped with Prestige Smart System (HDI, Home Diagnostics, Inc.). In animals receiving AAC, STZ injection was given 2 weeks after AAC. Animals were monitored every week using

glucose reagent strips for urine, Keto-Diastix (Bayer, Elkhart, IN). Animals with urine glucose levels above 250 mg/dl were allowed to continue in the experiment. Blood glucose was last measured at time of sacrifice.

Hemodynamic measurements. Blood pressure and LV pressure were measured in anesthetized animals. Animals received ketamine (80-100 mg/kg) plus Xyalazine (5 mg/kg) ip. When adequate anesthesia was achieved, a Millar catheter model SPR-671 was placed in the right common carotid artery for direct measurement of carotid mean arterial pressure (CMAP). After hemodynamic stabilization, the Millar catheter was advanced to the LV cavity in order to obtain direct measurements of LV pressures. An electrocardiogram (ECG) was recorded simultaneously. Data acquisition was performed using the MP 100 system from BIOPAC Systems, Inc., and analyzed using AcqKnowledge software.

Echocardiographic-doppler studies. Echocardiography with simultaneous monitoring of the arterial pressure was performed in anesthetized animals. Animals were anesthetized ip with ketamine (80-100 mg/kg) plus Xyalazine (5 mg/kg) and placed on a 37° C heating pad on left lateral decubitus. After hemodynamic stabilization, echocardiography was performed with a Sonos 5500 echocardiogram (Agilent Technologies, MA), equipped with a high-frequency intraoperative linear array transducer (21390 Agilent Technologies). Echocardiographic determinations were performed based upon the previously described technique⁹¹.

Left ventricular end-diastolic dimension (LVEDD), left ventricular end-systolic dimension (LVESD), septal (IVS) and posterior wall thickness (PWT) were measured by 2-dimension guided M-mode echocardiography from the parasternal long axis view obtained at the level of the papillary muscles. In addition, Doppler of the LV outflow at the aortic valve level was also obtained in order to measure ejection time (EjT) and the RR interval.

Systolic function was evaluated by the calculation of endocardial fractional shortening and rate-corrected velocity of circumferential shortening (VCFr). First, endocardial fractional shortening was calculated using the following equation:

$$(LVEDD-LVESD)/LVEDD \times 100$$

In addition, LV systolic chamber function was assessed from the rate-corrected (VCFr) using the following equation:

$$(LVEDD-LVESD/LVEDD)/(EjT-RR^{0.5})$$

The assessment of the circumferential systolic stress was performed with the simultaneous recording of the mean arterial pressure in the right carotid artery. It was calculated using the following equation:

$$\frac{P \cdot (LVESD/2)^2 [1 + (LVESD/2+PW_s)^2 / (LVESD/2+PW_s/2)^2]}{(LVESD/2+PW_s)^2 - (LVESD/2)^2}$$

Where P = Mean Arterial Pressure and PW_s = Posterior wall in systole

We used MAP for P, because MAP correlates closely with end-systolic pressure⁹¹. VCFr was normalized to circumferential stress by comparison with a stress-VCFr curve generated by linear regression of VCFr versus circumferential stress in control animals.

In addition to functional evaluation of the heart, echocardiography was used for calculation of left ventricular mass (LVM) and relative wall thickness (RWT).

LVM was calculated using a standard cube formula that assumes a spherical LV geometry⁵⁵ using the following equation:

$$1.04 \times [LVEDD + PWT + IVS]^3 - LVEDD^3].$$

In addition, relative wall thickness (RWT) was calculated as follows:

$$2PW/LVEDD$$

Determination of volume percent collagen. After hemodynamic and echocardiographic evaluation animals were sacrificed, then perfused with 0.9% saline for 10 minutes followed by buffered formalin or, in some experiments, immersion-fixed. The hearts were then dissected and right ventricular, LV - septum weights, and total heart weight (HW) were recorded. Both total and regional HW were normalized to body weight and the ratios compared among groups. Sections of the left ventricles were dehydrated through an ethanol series and embedded in paraffin. Serial sections (5 μ) were stained with hematoxylin-eosin for general morphology and picric acid-sirius red for collagen determination. LV cross-sections were digitized using a 10x objective of an IMT-2 inverted microscope (Olympus, Tokyo, Japan) equipped with a SPOT digital camera (Diagnostic Instruments). Images were after analyzed using Image Pro Plus (Media Cybernetics, Silver Springs, MD). The volume percent collagen was determined for 20-30 fields for each transmural region (subendomyocardial, subepimyocardial) and the mean value was calculated for each region, as well as for total myocardium.

Immunohistochemistry. Hearts from S. D. H. and H-D animals were frozen. LV sections were prepared and fixed in acetone for 10 minutes at -20°C . After blocking with 10% BSA for 30 minutes, slides were incubated with primary antibodies in 5% goat serum in PBS overnight at 4°C , followed by 3 stringent washes in PBS. The following primary antibodies was used: Collagen type I and type III (1:1000 and 1:150, respectively, AbCam). Sections were detected with ALEX448-conjugated, secondary antibodies (1:300, Molecular Probes). Measurements were performed on TIFF images obtained from representative photographs taken with a Spot Jr. digital camera (10 μm resolution) attached to an Olympus epifluorescent microscope.

Statistical Analysis. Results were expressed as mean \pm SEM. Differences among groups were evaluated by Statistical analysis performing one- or two-way analysis of variance (ANOVA). When F values are significant at a 95% confidence limit, differences among group means will be evaluated using Student Newman-Kuels or Bonferroni post-test procedure with a $p < 0.05$ considered significant.

Correlations between continuous parameters were determined from linear regression. All statistics were calculated by using SigmaStat statistical software (Jandel Scientific).

RESULTS

General characteristics of the animal groups. D was confirmed by the finding of serum glucose levels above 250mg/dl after 7 days post-STZ injection. Both D and H-D animals at 6 and 12 weeks had significant elevations ($p < 0.005$) of serum glucose when compared to S and or H. There were no significant differences in the H group (Tables 1 and 2).

D animals failed to gain weight after STZ injection. D and H-D groups had lower body weights ($p < 0.005$) at the end of the experiment when compare to S and H animals. However, body weight did not differ among the STZ-injected groups. In addition, D animals had lower HW when compared to S and H animals at 6 and 12 weeks. HW also was reduced in H-D animals when compared to S and HTN animals (Tables 3 and 4).

Hemodynamic measurements. Anesthetized measurements showed that MAP was significantly decreased ($p < 0.001$) in D group at 4 and 12 weeks when compared to S and H. In addition, there were significant elevations ($p < 0.001$) of MAP in the HTN animals at 6 and 12 weeks. Conversely, H-D animals did not present an elevation in MAP when compared to S. However, there was a statistically significant increase in MAP when compared to D at 4 and 12 weeks.

Table 1. Echocardiographic Measurements of S,D, H, and H-D Animals at 4 and 6 weeks.

	S	D	H	H-D
Time point	6 weeks	4 weeks	6 weeks	6 weeks
Echocardiography, <i>n</i>	10	16	15	9
MAP, mmHg	123±3	96=4*σ	151±5*φδ	122.1±52σφ
PW, mm	1.2±0.01	1.1=0.01*σ	1.4±0.05	1.2±0.05
IVS, mm	1.2±0.02	1.1±0.01σ	1.4±0.05	1.1±0.05σ
LVEDD, mm	7.2±0.17	7.7±0.12	7.3±0.13	6.87±0.19φ
LVESD, mm	3.0±0.19	4.3±0.12*σξ	3.3±0.06	3.2±0.06φ
RWT	0.3±0.37	0.2±0.31*σγξ	0.3±0.46	0.3±0.38
VCFr	3.1±0.11	2.2±0.09*σξδ	2.9±0.08	2.5±0.09*σ
VCFdif	0.0±0.04	-0.3±0.0*σδξ	0.0±0.07	-0.3±0.06*σδξ
Glucose, mg dl	151±7	370±20*σ	162±7	522±30*σδξ

Values are mean ± SEM. * ($p < 0.005$) vs. S at 6 weeks. δ ($p < 0.005$) vs. S 12 weeks. σ ($p < 0.005$) vs. H at 6 weeks. ξ ($p < 0.005$) vs H at 12 weeks. φ ($p < 0.05$) vs. D at 4 weeks. γ ($p < 0.005$) vs. H-D at 6 weeks.

Table 2. Echocardiographic Measurements of S,D, H, and H-D Animals at 12 weeks.

	S	D	H	H-D
Time point	12 weeks	12 weeks	12 weeks	12 weeks
Echocardiography, <i>n</i>	6	9	6	9
MAP, mmHg	117±7	96=3*	145=8φσ	120=6ξφσ
PW, mm	1.3±0.05	1.1±0.03ξ	1.5±0.12φ	1.3±0.09
IVS, mm	1.2±0.04	1.1±0.03ξ	1.5±0.1φ	1.2±0.08ξ
LVEDD, mm	7.7±0.2	7.6±0.06	7.2±0.1δ	7.8±0.3γ
LVESD, mm	3.7±0.34	4.6±0.19*σξδγ	3.4±0.2	4.3±0.2*ξσγ
RWT	0.3±0.01	0.3±0.0ξ	0.4±0.08	0.3±0.02ξ
VCFr	2.9±0.2	2.2±0.11*δξσ	2.8±0.1	2.3±0.10*δξσ
VCFdif	0.1±0.12	-0.3±0.05*σδ	0.0±0.10	-0.16±0.1*
Glucose, mg/dl	160±9	429±29*χδ	164±10	461±25*δξσ

Values are mean ± SEM. * ($p < 0.005$) vs. S at 6 weeks. δ ($p < 0.005$) vs. S 12 weeks. σ ($p < 0.005$) vs. H at 6 weeks. ξ ($p < 0.005$) vs H at 12 weeks. φ ($p < 0.05$) vs. D at 4 weeks. γ ($p < 0.005$) vs. H-D at 6 weeks.

Left ventricular remodeling. Measurements corresponding to posterior wall thickness (PWT), (IVS), LVEDD, and LVESD are summarized in Tables 1 and 2. The calculated RWT (2PW/LVEDD) showed that H animals presented an increase in this ratio when compared to S at 6 and 12 weeks, suggesting the presence of LVH as a compensatory mechanism in response to the AAC. In addition, RWT was decreased in the D group, suggesting the presence of cardiac dilatation, being significant at 4 and 12 weeks. However, RWT did not differ between D animals at 4 and 12 weeks.

Table 3. Body and heart weights obtained from S,D, H, and H-D animals at 4 and 6 weeks. HW and LV were normalized to body weight (BW) for all groups.

	S	D	H	H-D
Time point	6 weeks	4 weeks	6 weeks	6 weeks
<i>n</i>	9	8	10	6
BW, gr	393±2	309±1*	337.8±2	226±1*σ
HV mg	1.1±0.03	1.0±0.04	1.3±0.1	0.7±0.05*σ
HW/BW mg/g	2.9±0.1	3.3±0.09	3.9±0.2*	3.4±0.1
LV/BW mg/g	2.1±0.08	2.3±0.06	2.9±0.2*	2.4±0.1

Values are mean ± SEM. * ($p < 0.005$) vs. S at 6 weeks. δ ($p < 0.005$) vs. S 12 weeks. σ ($p < 0.005$) vs. H at 6 weeks. ξ ($p < 0.005$) vs H at 12 weeks.

Furthermore, RWT in the HD did not differ from the S groups at 4 and 12 weeks. In addition, postmortem determination of HW/BW and LV/HW ratios showed the following results: First, D animals alone did not differ from S at 4 or 12 weeks. Second, both ratios were significantly increased in the HTP group at 6 weeks when compared to S, suggesting the progression of LVH (Table 1 and 2).

Table 4. Body and heart weights obtained from S,D, H, and H-D animals at 12 weeks. HW and LV were normalized to body weight (BW) for all groups.

	S	D	H	H-D
Time point	12 weeks	12 weeks	12 weeks	12 weeks
<i>n</i>	5	19	6	6
BW, gr	418±4	288±1δξ	423±2	261±1δξ
HV mg	1.4±0.1	0.9±0.06ξ	1.5±0.07*	0.9±0.05ξ
HW/BW mg/g	3.0±0.1	3.2±0.1	3.7±.2	3.9±0.2* δ
LV/BW mg/g	2.2±0.1	2.3±0.06	2.7±0.1	2.8±0.2

Values are mean ± SEM. * (p < 0.005) vs. S at 6 weeks. δ (p < 0.005) vs. S 12 weeks. σ (p < 0.005) vs. H at 6 weeks. ξ (p < 0.005) vs H at 12 weeks.

Table 5. Interstitial collagen deposition in the endocardium and epicardium of S,D,H, and H-D animals at 4 and 6 weeks.

	S	D	H	H-D
Time point	6 weeks	4 weeks	6 weeks	6 weeks
<i>n</i>	8	9	8	8
Endocardium volume%	1.03±0.09	1.8±0.1	3.1±0.5*	4.1±0.6*δ
Epicardium volume%	1.02±0.1	1.78±0.1	2.2±0.4	3.8±0.5*δ
Total volume %	1.04±0.1	1.7±0.1	2.7±0.4*	3.9±0.5*δ

Values are mean ± SEM. * (p < 0.005) vs. S at 6 weeks. δ (p < 0.005) vs. S 12 weeks.

Table 6. Interstitial collagen deposition in the endocardium and epicardium of S,D,H, and H-D animals at 12 weeks.

	S	D	H	H-D
Time point	12 weeks	12 weeks	12 weeks	12 weeks
<i>n</i>	5	9	7	8
Endocardium volume%	1.3±0.1	2.3±0.2	3.4±0.9	4.1±2.8*
Epicardium volume%	1.4±0.04	2.1±0.1	2.5±0.5	3.0±0.4*δ
Total volume %	1.3±0.07	2.2±0.1	2.9±0.1	3.6±0.7*

Values are mean ± SEM. * (p < 0.005) vs. S at 6 weeks. δ (p < 0.005) vs. S 12 weeks.

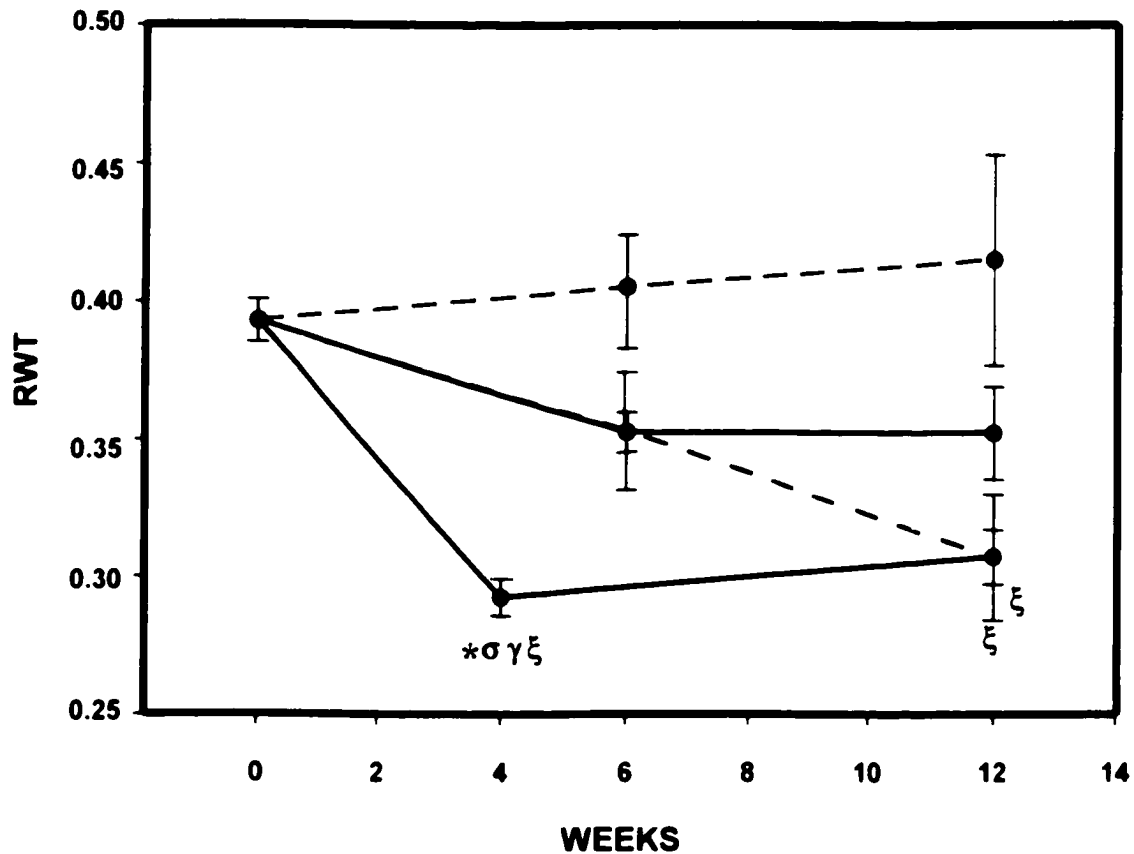


Figure 3. Temporal progression of RWT. RWT was calculated from $(2PW/LVEDD)$. Values corresponding posterior wall (PW) and left ventricular end-diastolic dimension (LVEDD) were determined by echocardiography at 4, 6, and 12 weeks in S, D, H, and H-D animals. Values are mean \pm SEM. * ($p < 0.005$) vs. S at 6 weeks. σ ($p < 0.005$) vs. H at 6 weeks. ξ ($p < 0.005$) vs. H at 12 weeks. γ ($p < 0.005$) vs. H-D at 6 weeks.

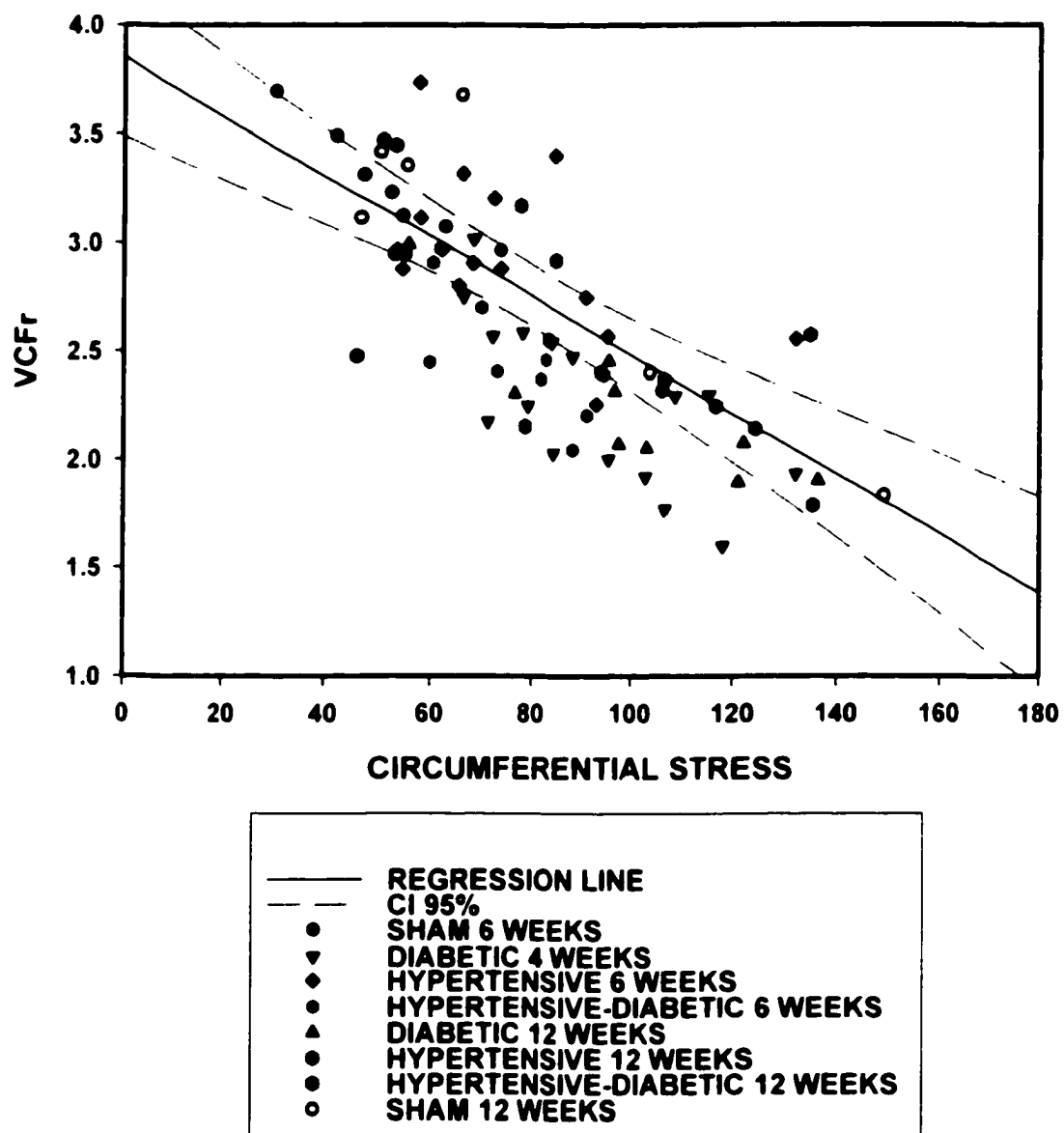


Figure 4. Relation of the velocity of circumferential shortening corrected for rate (VCFr) and circumferential stress. VCFr was determined from echocardiographic measurements. Circumferential stress was calculated using mean arterial pressure (MAP). Observed VCFr in each animal was compared to the VCFr predicted from the regression line for that level of circumferential stress.

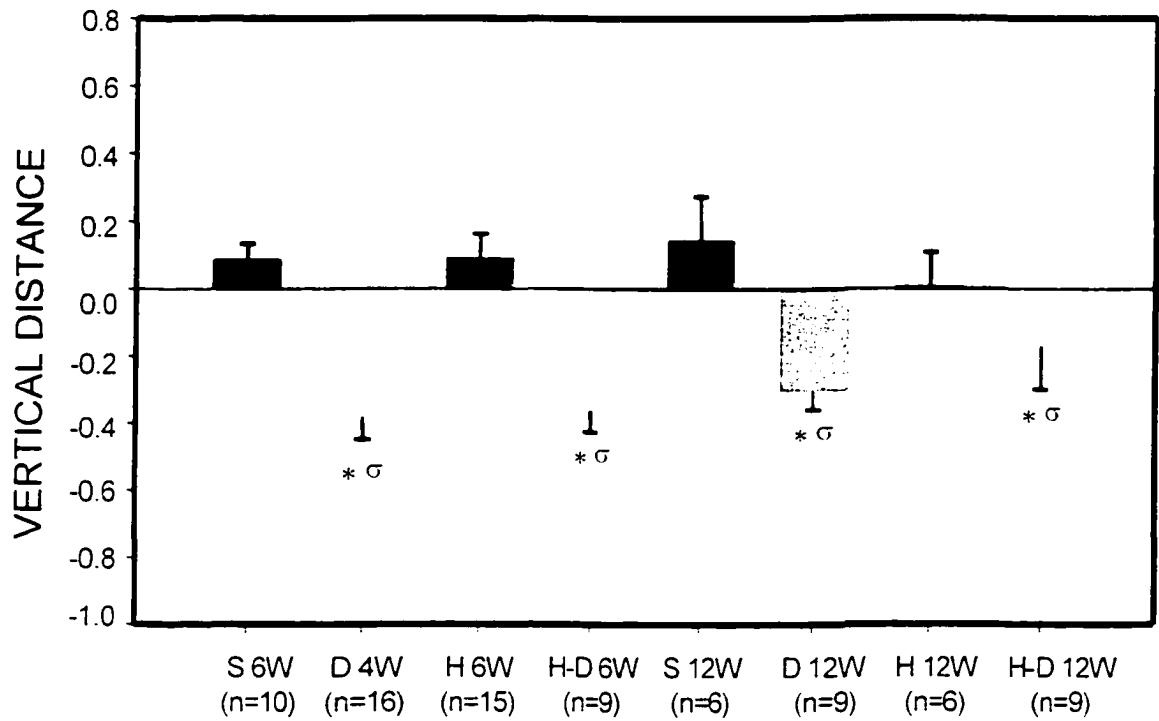


Figure 5. Calculated vertical distance (VD) from the regression line. VD was calculated for each rat and the mean for each group was determined. Values are mean \pm SEM.

* ($p < 0.005$) vs. S at 4 weeks. σ ($p < 0.005$) vs. H at 6 weeks.

However, H-D animals did not show a greater increase in HW/BW and LV/BW ratios when compared to HTN and D alone at both 6 and 12 weeks. Figure 3 shows the time-progression on RWT for each group.

Systolic function. Measurements corresponding calculated VCFr. VCFr corrected for stress vertical distances are summarized in Tables 1 and 2.

LV systolic function was decreased ($p < 0.005$) in D and H-D groups when compared to S and H at 6 and 12 weeks, as evidenced by a decreased echocardiographic VCFr. In addition, the VCFr was normalized to circumferential stress by comparison with a stress-VCFr curve generated by linear regression from control animals. When VCFr was corrected for differences in wall stress, the D group at both 4 and 12 weeks showed a significant reduction ($p < 0.005$) in systolic function when compared to S. However, there was no difference between the D group at 4 and 12 weeks (Figure 4).

On the other hand, H-D showed a decreased LV systolic function when compared to S at 6 and 12 weeks. However, there seems to be a moderate improvement in the H-D group at 12 weeks. There were no differences between D and H-D animals at any of the 2 time points studied. There were no differences between HTN animals and S at any time point.

Figure 4 shows the VCFr-stress curve generated by linear regression of VCFr versus circumferential stress in control animals and the VCFr observed for each rat. Figure 5 shows the mean VD calculated for each group.

Interstitial collagen deposition. Measurements corresponding to interstitial collagen deposition, including total, epicardium and endocardium, are summarized in Tables 5 and 6.

Total interstitial collagen was evaluated using picric acid-sirius red stain. Qualitative analysis indicated that the D group seemed to have a noticeable degree of interstitial collagen accumulation when compared to S (Figure 6). However, this difference did not reach statistical significance.

In addition, the presence of reactive fibrosis predominately in the endocardium was evident in the H and H-D groups at 4 and 12 weeks (Figure 7). On the other hand, H animals presented a significant increase in total collagen deposition when compared to S at 6 and 12 weeks. Furthermore, H-D animals presented the greatest increase in total collagen deposition at both 6 and 12 weeks ($p < 0.005$). However, there was no significant difference between D, H, and H-D groups at 6 and 12 weeks (Figure 8).

Figure 9 shows the temporal progression of total interstitial collagen deposition in all groups.

Immunohistochemistry. Qualitative evaluation of changes in collagen subtype deposition was performed by immunostaining. Results indicate that collagen I deposition, might be increased in the H and H-D group at 6 and 12 weeks. Additionally, there seems to be a change in collagen pattern throughout the myocardium with an apparent thickening of the collagen fibers (Figure 10). On the other hand, Collagen III changes suggest that there might be a reduction in collagen III in the D and H-D animals when

compared to S and H animals. In addition, alterations in the vascular bed appear to be present in the D and H-D animals at 4 and 12 weeks (Figure 11).

Figure 6. Changes in interstitial collagen deposition found in the diabetic hearts. Photomicrographs of cross section of endocardium. Paraffin-embedded sections of fixed left ventricles were stained with picric acid Sirius red and viewed at 10x magnification. A: S at 6 weeks. B: S at 12 weeks. C: D animals at 6 weeks. D: D animals at 12 weeks.

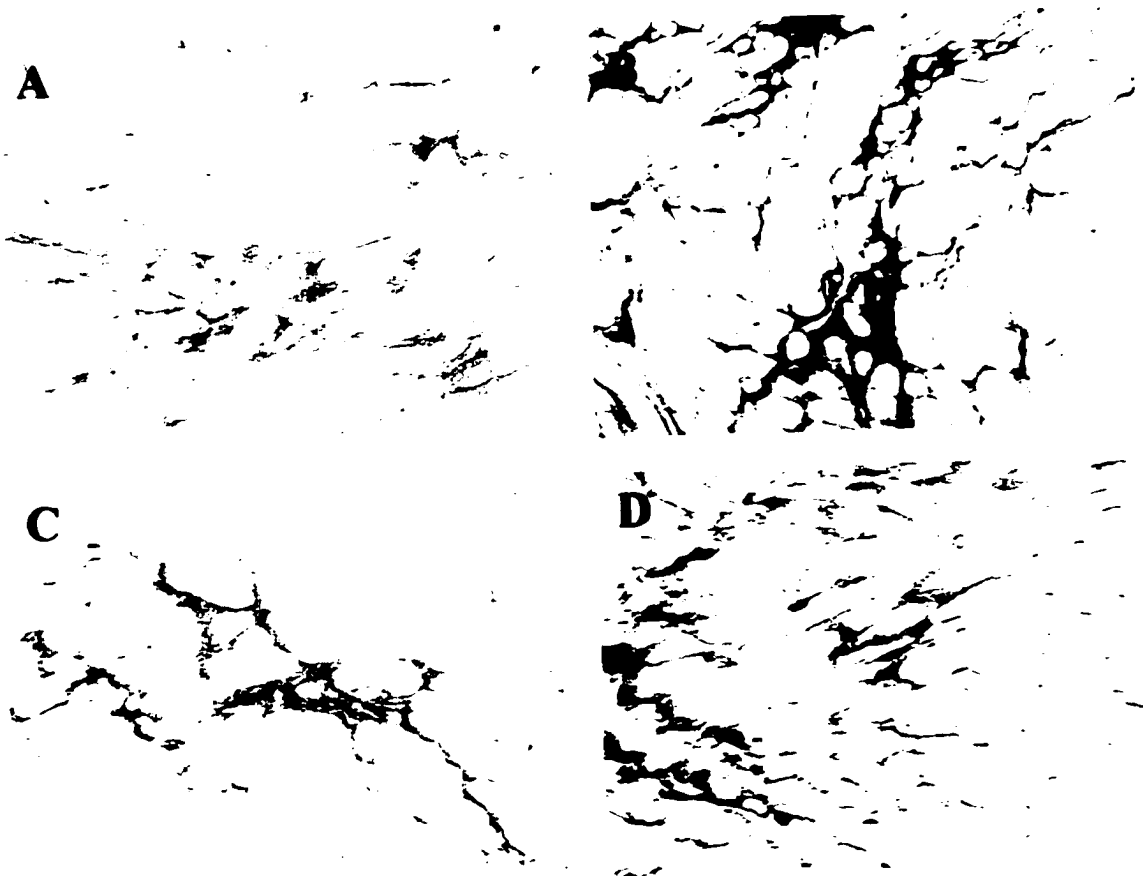
A

B

C

D

Figure 7. Focal fibrotic areas in the endocardium of H and H-D animals. Photomicrographs of cross section of endocardium. Paraffin-embedded sections of perfusion-fixed left ventricles were stained with picric acid Sirius red and viewed at 10x magnification. A: H animals at 6 weeks. B: H animals at 12 weeks. C: H-D animals at 6 weeks. D: H-D animals at 12 weeks.



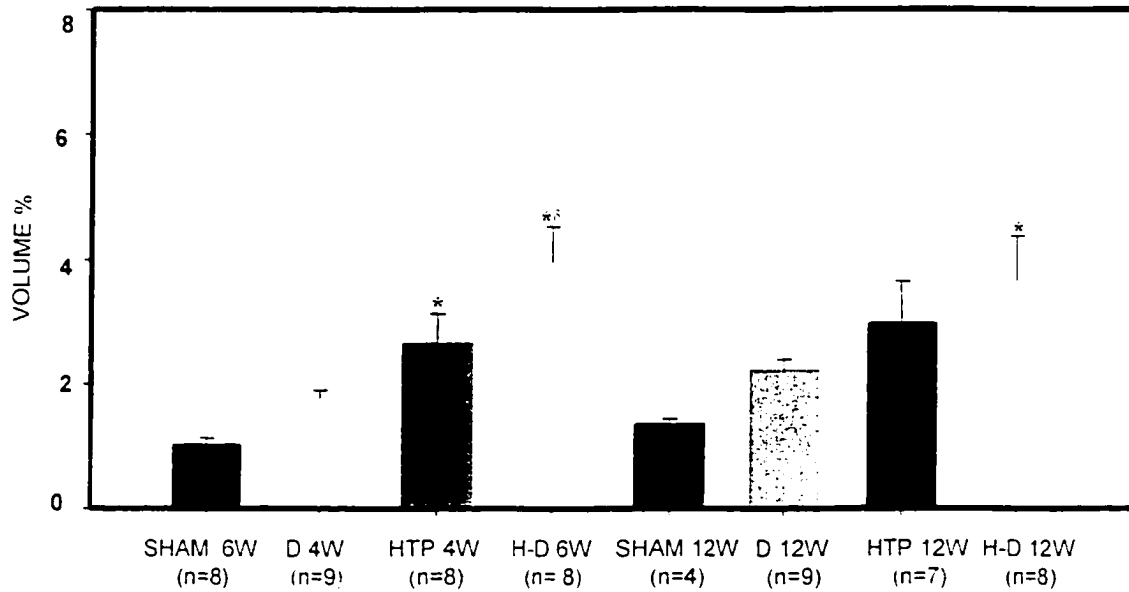


Figure 8. Total interstitial collagen deposition in the myocardium. Volume percent (%) of collagen was calculated from photomicrographs taken from paraffin-embedded cross section of left ventricular tissue stained with picric acid Sirius red. Photomicrographs were taken at 10x magnification and digitally analyzed. Collagen deposition was calculated for S, D, H, and H-D animals at 4, 6, and 12 weeks. Values are mean \pm SEM.

* ($p < 0.005$) vs. S at 6 weeks. δ ($p < 0.005$) vs. S at 12 weeks.

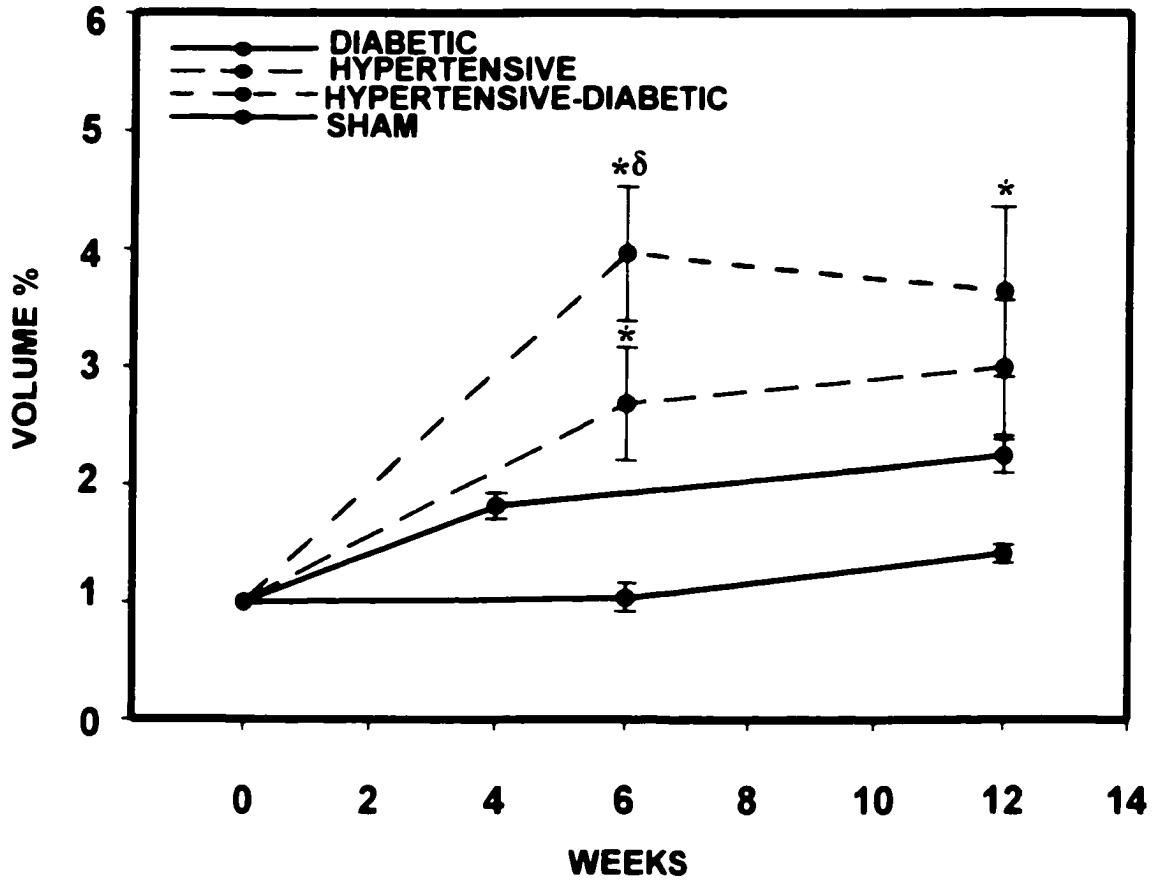


Figure 9. Temporal progression of interstitial collagen deposition in the myocardium. Volume percent (%) of interstitial collagen was calculated from photomicrographs taken from paraffin-embedded cross section of left ventricular tissue stained with picric acid Sirius red. Photomicrographs were taken at 10x magnification and digitally analyzed. Values are mean \pm SEM. * ($p < 0.005$) vs. S at 6 weeks. δ ($p < 0.005$) vs. S at 12 weeks.

Figure 10. Immunohistochemical staining of rat myocardium for collagen type I. Cardiac tissue was frozen, fixed with acetone, and stained with collagen type I primary antibody. Sections were detected with ALEX448-conjugated, secondary antibodies. Slides were analyzed at 40x magnification. A: S animal. B: D animal. C: H animal. D: H-D animal.

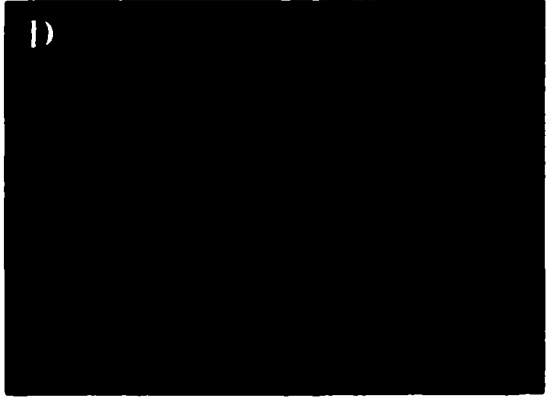
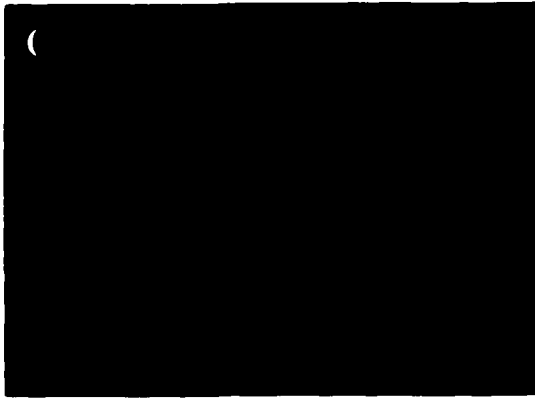
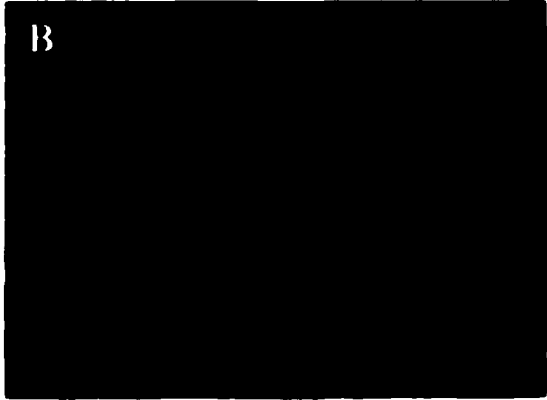
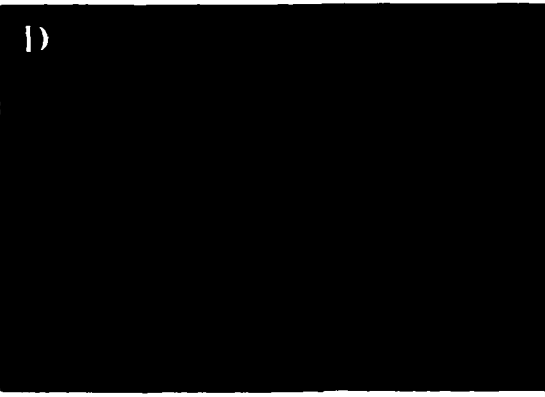
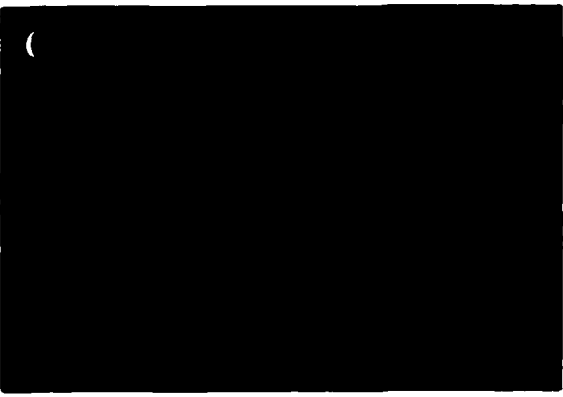
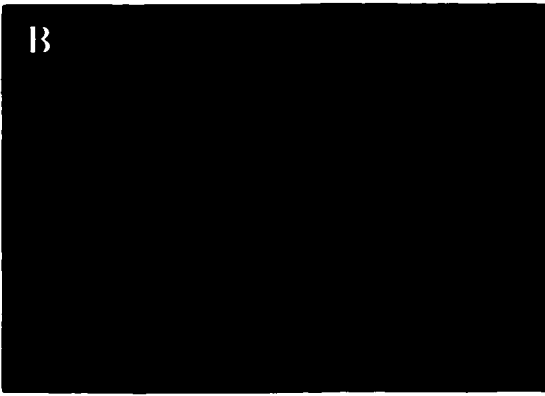
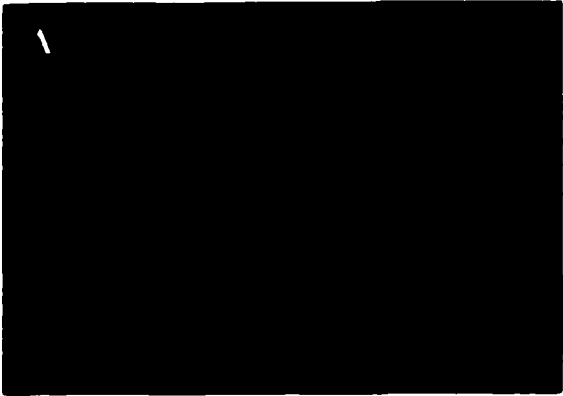


Figure 11. Immunohistochemical staining of rat myocardium for collagen type III. Cardiac tissue was frozen, fixed with acetone, and stained with collagen type III primary antibody. Sections were detected with ALEX448-conjugated, secondary antibodies. Slides were analyzed at 40x magnification. A: S animal. B: D animal. C: H animal. D: H-D animal.



DISCUSSION

Our results showed that hyperglycemia caused a significant impairment in systolic function at 4 and 12 weeks as evidenced by the significant reduction in the VCFr. In addition, adverse LV remodeling was evident at 4 weeks and persisted at 12 weeks. Diabetes produced an increase in interstitial collagen deposition at 4 and 12 weeks. In hypertensive animals, systolic function was unchanged after 6 and 12 weeks. However, H also resulted in LVH and increased collagen deposition that was evident at 6 and 12 weeks. The combination of D and H produced a significant impairment in systolic function at 6 and 12 weeks. However, no significant difference in systolic function was found between H-D animals and D animals. In addition, H-D animals presented the greatest degree of interstitial fibrosis, as well as replacement fibrosis at 6 and 12 weeks.

These results partially coincide with previous studies^{27,73} that also reported that the combination of both diseases caused the greatest degree of cardiac fibrosis. However, this is the first study to evaluate *in vivo* the temporal progression of cardiac remodeling and systolic function in response to HTN, DM, and H-D.

Our results indicated that H animals underwent LVH, as evidenced by an increase in RWT (2PW/LVEDD) and LV/BW and HW/BW ratio as early as 4 weeks. These results coincide with previous studies using the same experimental model, in which an increase in LV/BW ratio and wall thickness were also reported⁴⁷. These findings could be explained by the following pathophysiological mechanisms underlying LVH.

First, there is considerable increase in myocyte size, mainly cell diameter, resulting in cardiac hypertrophy⁹². This adaptive response normalizes wall stress and preserves cardiac function. Our results showed a preserved systolic function in hypertensive animals at 6 and 12 weeks.

Second, there is a progressive myocardial fibrosis⁷⁹, which has been linked to the degree of diastolic dysfunction. Myocardial fibrosis was evident in our study as the hypertensive animals presented an increase in interstitial collagen deposition at 6 and 12 weeks. These results can be partially explained by the activation of RAS and the increased secretion of Ang II in this experimental model using AAC⁹³. The hemodynamic and non-hemodynamic effects of angiotensin II are mostly mediated by the angiotensin II type I (AT₁) receptor, and it has been proposed that tissue growth factor β (TGF- β) mediates Ang II-induced fibrosis⁹⁴. Furthermore, there is now evidence that this fibrotic response is independent of the pressure effect and is mediated via neurohormonal mechanisms such as the RAS⁹⁵.

In addition, changes in the ECM components play an important role in maintaining chamber shape and myocyte alignment during LVH^{96,97}. ECM changes are regulated by MMPs which degrade fibrillar collagen and TIMPs maintaining an adequate balance between synthesis and degradation.

Previous studies have reported that the combined effects of DM and HTN in LV geometry result in a greater degree of LV hypertrophy and systolic dysfunction in individuals¹¹ and experimental models²⁷. Conversely, our results suggest that when HTH and DM were combined adverse ventricular remodeling seemed to occur at a slower rate than that seen in the diabetic hearts alone. Indeed, RWT (2PW/LVEDD) in H-D animals

did not differ from S at 6 weeks, but became significantly different at 12 weeks. However, LV systolic function remained impaired in both H-D hearts and diabetic hearts alone. Possible mechanisms underlying this systolic dysfunction will be discussed later.

We believe that this is a temporary response that would eventually progress to a more severe form of remodeling, leading to HF. In fact, it is possible that the hypertrophic response and subsequent increase in myocyte size counteract the myocyte apoptosis seen in the diabetic heart¹⁰⁴.

However, cardiac responses to hyperglycemia are still unclear. Our results showed that acute hyperglycemia resulted in an early (4 weeks) adverse LV remodeling that remained constant after 12 weeks. This adverse remodeling was evident by a significant LV wall thinning as well as a simultaneous LV chamber dilatation. Interestingly, this adverse dilatation and reduced systolic performance was evident in the absence of an increased afterload. Several mechanisms can be proposed for these changes.

Previous studies have reported that during acute hyperglycemia, there is an early increase in the apoptotic rate without evidence of cell necrosis⁹⁸. We believe that these changes in myocyte number and mass might have accounted for the adverse LV remodeling seen in the diabetic hearts. We also suspect that the reduction in the number of contractile units could partially explain the decreased systolic performance seen in the diabetic, as well as H-D hearts, as early as 4 weeks.

Additionally, as previously described, ECM components are indispensable in maintaining chamber architecture and myocyte alignment. In addition, it has been shown that MMPs and TIMPs are determinant factors during the progression of dilated

cardiomyopathy⁹⁹. However, little is known about the MMPs and TIMPs changes occurring in the diabetic heart. Furthermore, in cardiac fibrosis, changes in collagen type I and III ratio and collagen cross-linking in the diabetic heart are not well understood. It has been demonstrated that the non-enzymatic glycosylation of collagen can affect its interaction with cells, and other matrix components, and alter its cross-linking, thereby reducing collagen turnover and degradation¹⁰⁰.

Fibrosis development during DM, especially in the kidneys, has been closely related to the increased expression of TGF- β . In addition, our qualitative assessment of collagen subtypes suggested an increase in collagen type I in the diabetic and H-D hearts. On the other hand, collagen type III appeared to decrease in these two groups. These changes imply an imbalance between the flexibility and rigidity of the myocardial scaffolding, affecting LV geometry and, therefore, systolic chamber function. Although these preliminary results were obtained using qualitative techniques, other studies support these changes that occur during the progression of dilated cardiomyopathies, in which collagen type III decreases, collagen type I increases, and there is an alteration in collagen cross-linking⁹⁹. Taken together, it is possible that changes in the collagen ratio and reduced solubility due to DM may affect the modulation, activation, and action of MMPs and TIMPs, leading to an unbalanced synthesis-degradation process. This may result in an increase in the resistance of mature collagen to degradation, with lack of newly synthesized collagen. This might have accounted in part for the early interstitial fibrosis seen in the diabetic heart, at both early and late time points. In addition, it is possible that the fibrotic effects of TGF- β affect not only affect renal tissue¹⁰¹ but also the myocardium in the diabetic heart. Furthermore, the adverse cardiac remodeling evidenced

in our study could be associated with high levels of TGF- β , as elevated TGF- β levels have been found in late stages of dilated cardiomyopathy¹⁰².

Additionally, and consistent with previous reports⁷³, the present study confirmed that the most dramatic increase in interstitial collagen deposition was seen in the H-D animals.

Our study also showed the presence of replacement fibrosis areas predominately in the endocardium of H and H-D animals. It has been previously reported that hypertrophic hearts have an abnormal endocardium blood flow during acute stress events¹⁰³, increasing the vulnerability of the endocardium to ischemia during hypoperfusion. Thus, it is likely that during the presence of hyperglycemic stress, reduced endocardial blood flow might affect tissue perfusion and oxygenation, resulting in necrosis and later replacement fibrosis. On the other hand, studies have suggested that chronic hyperglycemia results in cardioprotection after ischemic-reperfusion injury, by making myocytes resistant to hypoxia-induced apoptosis and necrosis by preventing accumulation of Ca²⁺¹⁰⁴.

We conclude that hyperglycemia caused a significant impairment in systolic function with adverse LV remodeling. It also produced an increase in interstitial collagen deposition at 4 and 12 weeks. HTN resulted in LVH and increase collagen deposition. Additionally, the combination of DM and HTN produced the most severe degree of interstitial fibrosis, as well as replacement fibrosis.

These results have led us to hypothesize that the compensatory response triggered by high blood pressure and the activation of RAS may play a role in preserving LV geometry in the diabetic heart, protecting against the adverse LV dilatation seen during

diabetic cardiomyopathy. These mechanisms appear to be early and transitory phenomenon.

Our further studies should be focused on the following: First, identification of the fibrotic pathways underlying collagen accumulation in the diabetic heart. We believe that TGF- β might be a potential factor regulating collagen deposition in the diabetic hearts. Therefore, it is important to evaluate changes in TGF- β expression and its relation to collagen accumulation. Second, we must identify the role of collagen subtype changes and collagen cross-linking in the cardiac remodeling and systolic function. We believe that by identifying changes in collagen expression via mRNA we can elucidate some of our preliminary results.

REFERENCE LIST

- (1) American Heart Association. 2001 Heart and Stroke Statistical Update. Dallas, Texas: American Heart Association.
- (2) Laufer E, Jennings GL, Korner PI, Dewar E. Prevalence of cardiac structural and functional abnormalities in untreated primary hypertension. *Hypertension*. 1989; 13:151-162.
- (3) van Hoesven KH, Factor SM. A comparison of the pathological spectrum of hypertensive, diabetic, and hypertensive-diabetic heart disease. *Circulation*. 1990; 82:848-855.
- (4) Brilla CG, Maisch B. Regulation of the structural remodelling of the myocardium: from hypertrophy to heart failure. *Eur Heart J*. 1994;15 Suppl D:45-52.
- (5) Eleftheriades EG, Durand JB, Ferguson AG, Engelmann GL, Jones SB, Samarel AM. Regulation of procollagen metabolism in the pressure-overloaded rat heart. *J Clin Invest*. 1993;91:1113-1122.
- (6) Nathan DM. Long-term complications of diabetes mellitus. *N Eng J Med*. 1993; 328:1676-1685.
- (7) Harris MI, Flegal KM, Cowie CC, Eberhardt MS, Goldstein DE, Little RR, Wiedmeyer HM, Byrd-Holt DD. Prevalence of diabetes, impaired fasting glucose, and impaired glucose tolerance in U.S. adults. The Third National Health and Nutrition Examination Survey, 1988-1994. *Diabetes Care*. 1998;2:518-524.
- (8) Kannel WB, McGee DL. Diabetes and glucose tolerance as risk factors for cardiovascular disease: the Framingham study. *Diabetes Care*. 1979;2:120-126.
- (9) Barrett-Connor EL, Cohn BA, Wingard DL, Edelstein SL. Why is diabetes mellitus a stronger risk factor for fatal ischemic heart disease in women than in men? The Rancho Bernardo Study. *JAMA*. 1991;265:627-631.
- (10) Manson JE, Colditz GA, Stampfer MJ, Willett WC, Krolewski AS, Rosner B, Arky RA, Speizer FE, Hennekens CH. A prospective study of maturity-onset diabetes mellitus and risk of coronary heart disease and stroke in women. *Arch Intern Med*. 1991;151:1141-1147.
- (11) Bella JN, Devereux RB, Roman MJ, Palmieri V, Liu JE, Paranicas M, Welty TK, Lee ET, Fabsitz RR, Howard BV. Separate and joint effects of systemic

- hypertension and diabetes mellitus on left ventricular structure and function in American Indians (the Strong Heart Study). *Am J Cardio*. 2001;87:1260-1265.
- (12) Okayama H, Hamada M, Hiwada K. Contractile dysfunction in the diabetic-rat heart is an intrinsic abnormality of the cardiac myocyte. *Clinical Sci*. 1994;86:257-262.
- (13) Yu Z, Tibbits GF, McNeill JH. Cellular functions of diabetic cardiomyocytes: contractility, rapid-cooling contracture, and ryanodine binding. *Am J Physiol*. 1994;266:H2082-H2089.
- (14) Ganguly PK, Pierce GN, Dhalla KS, Dhalla NS. Defective sarcoplasmic reticular calcium transport in diabetic cardiomyopathy. *Am J Physiol*. 1983;244:E528-E535.
- (15) Wang DW, Kiyosue T, Shigematsu S, Arita M. Abnormalities of K^+ and Ca^{2+} -currents in ventricular myocytes from rats with chronic diabetes. *Am J Physiol*. 1995;269:H1288-H1296.
- (16) Shimoni Y, Ewart HS, Severson D. Insulin stimulation of rat ventricular K^+ -currents depends on the integrity of the cytoskeleton. *J Physiol*. 1999;51:735-745.
- (17) Casis O, Gallego M, Iriarte M, Sanchez-Chapula JA. Effects of diabetic cardiomyopathy on regional electrophysiologic characteristics of rat ventricle. *Diabetologia*. 2000;43:101-109.
- (18) Schaffer SW, Ballard-Croft C, Boerth S, Allo SN. Mechanisms underlying depressed Na^+/Ca^{2+} exchanger activity in the diabetic heart. *Cardiovas Res*. 1997;34:129-136.
- (19) Giles TD, Ouyang J, Kerut EK, Given MB, Allen GE, McIlwain EF, Greenberg SS. Changes in protein kinase C in early cardiomyopathy and in gracilis muscle in the BB/Wor diabetic rat. *Am J Physiol*. 1998;274:H295-H307.
- (20) Litwin SE, Raya TE, Anderson PG, Daugherty S, Goldman S. Abnormal cardiac function in the streptozotocin-diabetic rat. Changes in active and passive properties of the left ventricle. *J Clin Invest*. 1990;86:481-488.
- (21) Paulson DJ, Kopp SJ, Tow JP, Feliksik JM, Peace DG. Impaired in vivo myocardial reactivity to norepinephrine in diabetic rats. *Proc Society Exp Biol Med*. 1986;183:186-192.
- (22) Kashiwagi A, Nishio Y, Saeki Y, Kida Y, Kodama M, Shigeta Y. Plasma membrane-specific deficiency in cardiac beta-adrenergic receptor in streptozocin-diabetic rats. *Am J Physiol*. 1989;257:E127-E132.
- (23) Savarese JJ, Berkowitz BA. beta-Adrenergic receptor decrease in diabetic rat hearts. *Life Sci*. 1979;25:2075-2078.

- (24) Heller BA, Paulson DJ, Kopp SJ, Peace DG, Tow JP. Depressed in vivo myocardial reactivity to dobutamine in streptozotocin diabetic rats: influence of exercise training. *Cardiovas Res*. 1988; 22(6):417-424.
- (25) Smith JM, Paulson DJ, Romano FD. Inhibition of nitric oxide synthase by L-NAME improves ventricular performance in streptozotocin-diabetic rats. *J Molec & Cell Cardio*. 1997; 29:2393-2402.
- (26) Khaidar A, Marx M, Lubec B, Lubec G. L-arginine reduces heart collagen accumulation in the diabetic db/db mouse. *Circulation*. 1994;90:479-483.
- (27) Factor SM, Bhan R, Minase T, Wolinsky H, Sonnenblick EH. Hypertensive-diabetic cardiomyopathy in the rat: an experimental model of human disease. *Am J Path*. 1981;102:219-228.
- (28) Norton GR, Candy G, Woodiwiss AJ. Aminoguanidine prevents the decreased myocardial compliance produced by streptozotocin-induced diabetes mellitus in rats. *Circulation*. 1996;93:1905-1912.
- (29) Vlassara H. Recent progress on the biologic and clinical significance of advanced glycosylation end products. *J Lab & Clin Med*. 1994;124:19-30.
- (30) Penpargkul S, Schaible T, Yipintsoi T, Scheuer J. The effect of diabetes on performance and metabolism of rat hearts. *Circulation Res*. 1980;47:911-921.
- (31) Karnieli E, Armoni M, Cohen P, Kanter Y, Rafaeloff R. Reversal of insulin resistance in diabetic rat adipocytes by insulin therapy. Restoration of pool of glucose transporters and enhancement of glucose-transport activity. *Diabetes*. 1987;36:925-931.
- (32) Kobayashi M, Olefsky JM. Effects of streptozotocin-induced diabetes on insulin binding, glucose transport, and intracellular glucose metabolism in isolated rat adipocytes. *Diabetes*. 1979;28:87-95.
- (33) Kerbey AL, Vary TC, Randle PJ. Molecular mechanisms regulating myocardial glucose oxidation. *Basic Res Cardiol*. 1985;80 Suppl 2:93-96.
- (34) West KM, Ahuja MM, Bennett PH, Czyzyk A, De Acosta OM, Fuller JH, Grab B, Grabauskas V, Jarrett RJ, Kosaka K. The role of circulating glucose and triglyceride concentrations and their interactions with other "risk factors" as determinants of arterial disease in nine diabetic population samples from the WHO multinational study. *Diabetes Care*. 1983;6:361-369.
- (35) Solomon SS, Heckemeyer CM, Barker JA, Duckworth WC. Hormonal control of lipolysis in perfused adipocytes from diabetic rats. *Endocrinology*. 1985; 117:1350-1354.

- (36) Braun JE, Severson DL. Diabetes reduces heparin- and phospholipase C-releasable lipoprotein lipase from cardiomyocytes. *Am J Physiol.* 1991;260:E477-E485.
- (37) Havel RJ. Lipid transport and the availability of insulin. *Hormone & Metabolic Research* 1974;Suppl 4:51-53.
- (38) Rodrigues B, Ross JR, Farahbakshian S, McNeill JH. Effects of in vivo and in vitro treatment with L-carnitine on isolated hearts from chronically diabetic rats. *Can J Physiol & Pharmacol.* 1990;68:1085-1092.
- (39) Fields LE, Daugherty A, Bergmann SR. Effect of fatty acid on performance and lipid content of hearts from diabetic rabbits. *Am J Physiol.* 86:250:H1079-H1085.
- (40) Katz AM, Messineo FC. Lipid-membrane interactions and the pathogenesis of ischemic damage in the myocardium. *Circulation Res.*1981;48:1-16.
- (41) Cutler JA. High blood pressure and end-organ damage. *Journal of Hypertension - Supplement* 1996;14:S3-S6.
- (42) The sixth report of the Joint National Committee on prevention, detection, evaluation, and treatment of high blood pressure. *Arch Inter Med* 1997; 157:2413-2446.
- (43) Luft FC. Molecular genetics of human hypertension. *Current Opinion in Nephrology & Hypertension.* 2000;9:259-266.
- (44) Lifton RP. Genetic determinants of human hypertension. *Proc Natl Acad Sci U.S.A.* 1995;92:8545-8551.
- (45) Lifton RP. Molecular genetics of human blood pressure variation. *Science.* 1996; 272:676-680.
- (46) Fernandes M, Onesti G, Weder A, Dykyj R, Gould AB, Kim KE, Swartz C. Experimental model of severe renal hypertension. *J Lab & Clin Med.* 1976; 87:561-567.
- (47) Laurent D, Allergini PR, Zierhut W. Different left ventricular remodelling and function in two models of pressure overload as assessed in vivo by magnetic resonance imaging. *J Hypertens.* 1995; 1:693-700.
- (48) Frohlich ED, Tarazi RC, Dustan HP. Clinical-physiological correlations in the development of hypertensive heart disease. *Circulation.* 1971;44:446-455.
- (49) Inouye I, Massie B, Loge D, Topic N, Silverstein D, Simpson P, Tubau J. Abnormal left ventricular filling: an early finding in mild to moderate systemic hypertension. *Am J Cardiol.* 1984;53:120-126.

- (50) de Simone G, Devereux RB, Roman MJ, Ganau A, Saba PS, Alderman MH, Laragh JH. Assessment of left ventricular function by the midwall fractional shortening/end-systolic stress relation in human hypertension. *J Am Coll Cardiol*. 1994;23:1444-1451.
- (51) Blake J, Devereux RB, Borer JS, Szulc M, Pappas TW, Laragh JH. Relation of obesity, high sodium intake, and eccentric left ventricular hypertrophy to left ventricular exercise dysfunction in essential hypertension. *Ame J Med*. 1990;88:477-485.
- (52) Sobue T, Yokota M, Iwase M, Ishihara H. Influence of left ventricular hypertrophy on left ventricular function during dynamic exercise in the presence or absence of coronary artery disease. *J Am Coll Cardiol*. 1995; 25:91-98.
- (53) Fouad FM, Slominski JM, Tarazi RC. Left ventricular diastolic function in hypertension: relation to left ventricular mass and systolic function. *J Am College Cardiol*. 1984;3:1500-1506.
- (54) Ohkusa T, Hisamatsu Y, Yano M, Kobayashi S, Tatsuno H, Saiki Y, Kohno M, Matsuzaki M. Altered cardiac mechanism and sarcoplasmic reticulum function in pressure overload-induced cardiac hypertrophy in rats. *J Mole & Cell Cardiol*. 1997;29:45-54.
- (55) Litwin SE, Katz SE, Weinberg EO, Lorell BH, Aurigemma GP, Douglas PS. Serial echocardiographic-Doppler assessment of left ventricular geometry and function in rats with pressure-overload hypertrophy. Chronic angiotensin-converting enzyme inhibition attenuates the transition to heart failure. *Circulation*. 1995;91:2642-2654.
- (56) Cory CR, Grange RW, Houston ME. Role of sarcoplasmic reticulum in loss of load-sensitive relaxation in pressure overload cardiac hypertrophy. *Am J Physiol*. 1994;266:H68-H78.
- (57) Kim S, Iwao H. Molecular and cellular mechanisms of angiotensin II-mediated cardiovascular and renal diseases. *Pharmacol Rev*. 2000;52:11-34.
- (58) Lijnen P, Petrov V. Antagonism of the renin-angiotensin system, hypertrophy and gene expression in cardiac myocytes. *Meth & Find in Exp & Clin Pharmacol*. 1999;21:363-374.
- (59) Levy D, Anderson KM, Savage DD, Kannel WB, Christiansen JC, Castelli WP. Echocardiographically detected left ventricular hypertrophy: prevalence and risk factors. The Framingham Heart Study. *Ann Int Med*. 1988;108:7-13.
- (60) Liebson PR, Grandits G, Prineas R, Dianzumba S, Flack JM, Cutler JA, Grimm R, Stamler J. Echocardiographic correlates of left ventricular structure among 844 mildly hypertensive men and women in the Treatment of Mild Hypertension Study (TOMHS). *Circulation*. 1993;87:476-486.

- (61) Messerli FH, Sundgaard-Riise K, Reisin ED, Dreslinski GR, Ventura HO, Oigman W, Frohlich ED, Dunn FG. Dimorphic cardiac adaptation to obesity and arterial hypertension. *Ann Int Med.* 1983;99:757-761.
- (62) Hammond IW, Devereux RB, Alderman MH, Laragh JH. Relation of blood pressure and body build to left ventricular mass in normotensive and hypertensive employed adults. *J Am Coll Cardiol.* 1988; 12:996-1004.
- (63) Shapiro LM, Mackinnon J, Beevers DG. Echocardiographic features of malignant hypertension. *Br Heart J.* 1981;46:374-379.
- (64) Houghton JL, Frank MJ, Carr AA, von Dohlen TW, Prisant LM. Relations among impaired coronary flow reserve, left ventricular hypertrophy and thallium perfusion defects in hypertensive patients without obstructive coronary artery disease. *J Am Coll Cardiol.* 1990;15:43-51.
- (65) Messerli FH, Ventura HO, Elizardi DJ, Dunn FG, Frohlich ED. Hypertension and sudden death. Increased ventricular ectopic activity in left ventricular hypertrophy. *Am J Med.* 1984;77:18-22.
- (66) Borg TK, Caulfield JB. The collagen matrix of the heart. *Fed Proc.* 1981; 40:2037-2041.
- (67) Levy D, Anderson KM, Plehn J, Savage DD, Christiansen JC, Castelli WP. Echocardiographically determined left ventricular structural and functional correlates of complex or frequent ventricular arrhythmias on one-hour ambulatory electrocardiographic monitoring. *Am J Cardiol.* 1987;59:836-840.
- (68) National High Blood Pressure Education Program Working Group report on hypertension in diabetes. *Hypertension.* 1994; 23:145-158.
- (69) Pijl AJ, van der Wal AC, Mathy MJ, Kam KL, Hendriks MG, Pfaffendorf M, van Zwieten PA. Streptozotocin-induced diabetes mellitus in spontaneously hypertensive rats: a pathophysiological model for the combined effects of hypertension and diabetes. *J Pharmacol & Toxicol Meth.* 1994;32:225-233.
- (70) Regan TJ. Congestive heart failure in the diabetic. *Ann Rev Med.* 1983;34:161-168.
- (71) Venco A, Grandi A, Barzizza F, Finardi G. Echocardiographic features of hypertensive-diabetic heart muscle disease. *Cardiology.* 1987;74:28-34.
- (72) Gress TW, Nieto FJ, Shahar E, Wofford MR, Brancati FL. Hypertension and antihypertensive therapy as risk factors for type 2 diabetes mellitus. Atherosclerosis Risk in Communities Study. *N Engl J Med.* 2000; 342:905-912.

- (73) Fein FS, Cho S, Zola BE, Miller B, Factor SM. Cardiac pathology in the hypertensive diabetic rat. Biventricular damage with right ventricular predominance. *Am J Pathol*. 1989;134:1159-1166.
- (74) Fein FS, Zola BE, Malhotra A, Cho S, Factor SM, Scheuer J, Sonnenblick EH. Hypertensive-diabetic cardiomyopathy in rats. *Am J Physiol*. 1990;258:H793-H805.
- (75) Alpert MA, Terry BE, Lambert CR, Kelly DL, Panayiotou H, Mukerji V, Massey CV, Cohen MV. Factors influencing left ventricular systolic function in nonhypertensive morbidly obese patients, and effect of weight loss induced by gastroplasty. *Am J Cardiol*. 1993;71:733-737.
- (76) Factor SM, Minase T, Sonnenblick EH. Clinical and morphological features of human hypertensive-diabetic cardiomyopathy. *Am Heart J*. 1980; 99:446-458.
- (77) Dwyer EM, Asif M, Ippolito T, Gillespie M. Role of hypertension, diabetes, obesity, and race in the development of symptomatic myocardial dysfunction in a predominantly minority population with normal coronary arteries. *Am Heart J*. 2000; 39:297-304.
- (78) Brilla CG, Matsubara L, Weber KT. Advanced hypertensive heart disease in spontaneously hypertensive rats. Lisinopril-mediated regression of myocardial fibrosis. *Hypertension*. 1996;28:269-275.
- (79) Brilla CG, Funck RC, Rupp H. Lisinopril-mediated regression of myocardial fibrosis in patients with hypertensive heart disease. *Circulation*. 2000;102:1388-1393.
- (80) Hamby RI, Zoneraich S, Sherman L. Diabetic cardiomyopathy. *JAMA*. 1974; 229:1749-1754.
- (81) Grossman E, Shemesh J, Shamiss A, Thaler M, Carroll J, Rosenthal T. Left ventricular mass in diabetes-hypertension. *Arch Int Med*. 1992; 152:1001-1004.
- (82) Mizushige K, Yao L, Noma T, Kiyomoto H, Yu Y, Hosomi N, Ohmori K, Matsuo H. Alteration in left ventricular diastolic filling and accumulation of myocardial collagen at insulin-resistant prediabetic stage of a type II diabetic rat model. *Circulation*. 2000;101(8):899-907.
- (83) Factor SM, Minase T, Cho S, Fein F, Capasso JM, Sonnenblick EH. Coronary microvascular abnormalities in the hypertensive-diabetic rat. A primary cause of cardiomyopathy? *Am J Pathol*. 1984;116:9-20.
- (84) Sowers JR, Standley PR, Ram JL, Jacober S, Simpson L, Rose K. Hyperinsulinemia, insulin resistance, and hyperglycemia: contributing factors in the pathogenesis of hypertension and atherosclerosis. *Am J Hypertens*. 1993;6:260S-270S.

- (85) Sowers JR, Sowers PS, Peuler JD. Role of insulin resistance and hyperinsulinemia in development of hypertension and atherosclerosis. *J Lab & Clin Med.* 1994; 123:647-652.
- (86) Hii PA, Rasmussen SM. Transcapillary escape rate of albumin and plasma volume in short- and long-term juvenile diabetics. *Scandinavian J Clin & Lab Invest.* 1973;32:81-87.
- (87) Joyner WL, Mayhan WG, Johnson RL, Phares CK. Microvascular alterations develop in Syrian hamsters after the induction of diabetes mellitus by streptozotocin. *Diabetes.* 1981;30:93-100.
- (88) Levy J, Gavin JR, III, Sowers JR. Diabetes mellitus: a disease of abnormal cellular calcium metabolism? *Am J Med.* 1994;96:260-273.
- (89) Nadler JL, Malayan S, Luong H, Shaw S, Natarajan RD, Rude RK. Intracellular free magnesium deficiency plays a key role in increased platelet reactivity in type II diabetes mellitus. *Diabetes Care.* 1992;15:835-841.
- (90) Okamura T, Miyazaki M, Inagami T, Toda N. Vascular renin-angiotensin system in two-kidney, one clip hypertensive rats. *Hypertension.* 1986;8:560-565.
- (91) Perry GJ, Mori T, Wei CC, Xu XY, Chen YF, Oparil S, Lucchesi P, Dell'Italia LJ. Genetic variation in angiotensin-converting enzyme does not prevent development of cardiac hypertrophy or upregulation of angiotensin II in response to aortocaval fistula. *Circulation.* 2001;103:1012-1016.
- (92) Swynghedauw B. Remodelling of the heart in response to chronic mechanical overload. *Euro Heart J.* 1989;10:935-943.
- (93) Nishimura M, Milsted A, Block CH, Brosnihan KB, Ferrario CM. Tissue renin-angiotensin systems in renal hypertension. *Hypertension.* 1992;20:158-167.
- (94) Mezzano SA, Ruiz-Ortega M, Egido J. Angiotensin II and renal fibrosis. *Hypertension.* 2001;38:635-638.
- (95) Brilla CG. Regression of myocardial fibrosis in hypertensive heart disease: diverse effects of various antihypertensive drugs. *Cardiovas Res.* 2000;46:324-331.
- (96) Weber KT, Anversa P, Armstrong PW, Brilla CG, Burnett JC, Jr., Cruickshank JM, Devereux RB, Giles TD, Korsgaard N, Leier CV. Remodeling and reparation of the cardiovascular system. *J Am Coll Cardiol.* 1992;20:3-16.
- (97) Robinson TF, Cohen-Gould L, Factor SM. Skeletal framework of mammalian heart muscle. Arrangement of inter- and pericellular connective tissue structures. *Lab Invest.* 1983;49:482-498.

- (98) Fiordaliso F, Li B, Latini R, Sonnenblick EH, Anversa P, Leri A, Kajstura J. Myocyte death in streptozotocin-induced diabetes in rats in angiotensin II-dependent. *Lab Invest*. 2000;80:513-527.
- (99) Gunja-Smith Z, Morales AR, Romanelli R, Woessner JF, Jr. Remodeling of human myocardial collagen in idiopathic dilated cardiomyopathy. Role of metalloproteinases and pyridinoline cross-links. *Am J Pathol*. 1996;148:1639-1648.
- (100) Paul RG, Bailey AJ. Glycation of collagen: the basis of its central role in the late complications of ageing and diabetes. *Internat J Biochem & Cell Biol*. 1996;28:1297-1310.
- (101) Gaedeke J, Peters H, Noble NA, Border WA. Angiotensin II, TGF-beta and renal fibrosis. *Contrib to Nephrol*. 2001;(135):153-160.
- (102) Holweg CT, Baan CC, Niesters HIG, Vantrimpont PJ, Mulder PG, Maat AP, Weimar W, Balk AH. TGF-beta1 gene polymorphisms in patients with end-stage heart failure. *J Heart & Lung Transplant* 2001;20:979-984.
- (103) Vrobel TR, Ring WS, Anderson RW, Emery RW, Bache RJ. Effect of heart rate on myocardial blood flow in dogs with left ventricular hypertrophy. *Am J Physiol*. 1980;239:H621-H627.
- (104) Schaffer SW, Croft CB, Solodushko V. Cardioprotective effect of chronic hyperglycemia: effect on hypoxia-induced apoptosis and necrosis. *Am J Physiol*. 2000;278:H1948-H1954.

APPENDIX

INSTITUTIONAL ANIMAL CARE AND USE COMMITTEE APPROVAL FORM

NOTICE OF APPROVAL

DATE: November 2, 2001

TO: Kathleen H. Bardeck, Ph.D.
MCLM-988-0005
FAX: 934-1445

FROM: Clinton J. Grubbs, Ph.D., Chairman 
Institutional Animal Care and Use Committee

SUBJECT: The Renin-Ang II System in Cardiovascular Remodeling (NIH) 011105822

On November 2, 2001, the University of Alabama at Birmingham Institutional Animal Care and Use Committee (IACUC) reviewed the animal use proposed in the above referenced application. It approved the use of the following species and numbers of animals:

Species	Use Category	Number in Category
Rats	B	350

Animal use is scheduled for review one year from November 2, 2001. Approval from the IACUC must be obtained before implementing any changes or modifications in the approved animal use.

Please keep this record for your files, and forward the attached letter to the appropriate granting agency.

Refer to Animal Protocol Number (APN) 011105822 when ordering animals or in any correspondence with the IACUC or Animal Resources Program (ARP) offices regarding this study. If you have concerns or questions regarding this notice, please call the IACUC office at 934-7592.

**GRADUATE SCHOOL
UNIVERSITY OF ALABAMA AT BIRMINGHAM
THESIS APPROVAL FORM**

Degree M.S.B.M.S. **Graduate Program** Physiology and Biophysics

Name of Candidate Juan M. Bernal

Title of Thesis Cardiac Remodeling and Systolic Function in Response
 to Hypertension (HTN), Diabetes (D), and Hypertension-
 Diabetes (H-D)

I certify that I have read this document and examined the student regarding its content. In my opinion, this thesis conforms to acceptable standards of scholarly presentation and is adequate in scope and quality, and the attainments of this student are such that he may be recommended for the master's degree.

Thesis Committee:

Name		Signature
<u> Kathleen H. Berecek </u>	Co-Chair	<u> Kathleen H. Berecek </u>
<u> Pamela A. Lucchesi </u>	Co-Chair	<u> Pamela A. Lucchesi </u>
<u> Gilbert J. Perry </u>		<u> Gilbert J. Perry </u>
<u> Louis J. Dell'Italia </u>		<u> Louis J. Dell'Italia </u>
<u> C. Roger White </u>		<u> C. Roger White </u>

Director of Graduate Program M. Scicibò

Dean, UAB Graduate School _____

Date 6/5/02